

REPORT DOCUMENTATION PAGE			Form Approved OMB No. 0704-0188		
Public reporting burden for this collection of information is estimated to average 1 hour per response, including the time for reviewing instructions, searching existing data sources, gathering and maintaining the data needed, and completing and reviewing this collection of information. Send comments regarding this burden estimate or any other aspect of this collection of information, including suggestions for reducing this burden to Department of Defense, Washington Headquarters Services, Directorate for Information Operations and Reports (0704-0188), 1215 Jefferson Davis Highway, Suite 1204, Arlington, VA 22202-4302. Respondents should be aware that notwithstanding any other provision of law, no person shall be subject to any penalty for failing to comply with a collection of information if it does not display a currently valid OMB control number. PLEASE DO NOT RETURN YOUR FORM TO THE ABOVE ADDRESS.					
1. REPORT DATE (DD-MM-YYYY) 06-04-2012		2. REPORT TYPE STTR Ph II Final Report		3. DATES COVERED (From - To) 01 DEC 2009 - 31 MAR 2012	
4. TITLE AND SUBTITLE Orthogonal Chip Based Electronic Sensors for Chemical Agents			5a. CONTRACT NUMBER FA9550-10-C-0019		
			5b. GRANT NUMBER		
			5c. PROGRAM ELEMENT NUMBER		
6. AUTHOR(S) Sanjay V. Patel, Ph.D.			5d. PROJECT NUMBER		
			5e. TASK NUMBER		
			5f. WORK UNIT NUMBER		
7. PERFORMING ORGANIZATION NAME(S) AND ADDRESS(ES) Seacoast Science Inc. 2151 Las Palmas Dr. Suite C Carlsbad, CA 92011			8. PERFORMING ORGANIZATION REPORT NUMBER 01		
9. SPONSORING / MONITORING AGENCY NAME(S) AND ADDRESS(ES) USAF, AFRL, AF OFFICE OF SCIENTIFIC RESEARCH 875 Randolph Street Room 3112 Arlington, VA 22203			10. SPONSOR/MONITOR'S ACRONYM(S) USAF, AFRL, AFOSR/RSE		
			11. SPONSOR/MONITOR'S REPORT NUMBER(S) AFRL-OSR-VA-TR-2012-1046		
12. DISTRIBUTION / AVAILABILITY STATEMENT DISTRIBUTION STATEMENT A: Approved for public release; distribution is unlimited					
13. SUPPLEMENTARY NOTES					
14. ABSTRACT Seacoast Science, Inc. and the University of California, San Diego (UCSD) are developing a portable real-time chemical detector system containing multiple sensor technologies. This Phase II STTR final report details our accomplishments during the 2-year program. Scientists at UCSD have modeled the behavior of the metal-phthalocyanine ChemFET, and optimizing both the sensor chemistry and methods to understand the sensor data. Seacoast Science has developed a packed-tube, trap-and-purge preconcentrator to collect vapor samples, with the goal of improving the sensitivity of the ultimate sensor system. Increased sensitivity allows for improved signal to noise for pattern recognition and for better protection for the warfighters who will use the system. In Phase II, Seacoast developed and tested an integrated prototype, integrating both the UCSD chemFET array and Seacoast's chemicapacitor array with the preconcentrator. UCSD has developed methods for solution deposition of sensor films using soluble phthalocyanines. Development of the preconcentrator and sensor materials demonstrate Seacoast's leading-edge sensor systems for chemical threats of critical importance to the US military. Improvements in the systems developed under this program are being integrated into Seacoast's Mini GC product prototypes for vapor detection for applications such as environmental contamination detection and aerosol analysis.					
15. SUBJECT TERMS SBIR Report, chemFET, chemicapacitor array, preconcentrator, detection, electronic sensors, chemical agents					
16. SECURITY CLASSIFICATION OF:			17. LIMITATION OF ABSTRACT UU	18. NUMBER OF PAGES 33	19a. NAME OF RESPONSIBLE PERSON Sanjay V. Patel
a. REPORT U	b. ABSTRACT U	c. THIS PAGE U			19b. TELEPHONE NUMBER (include area code) 760-268-0083 ext:15

Orthogonal Chip Based Electronic Sensors for Chemical Agents

Phase II Final Technical Report: April 06, 2012

Period of Performance: 1 Dec. 2009 through 31 March 2012

AFOSR STTR Phase II Contract Number: FA9550-10-C-0019

Distribution Statement A. Approved for public release; distribution is unlimited.

Principal Investigator: Sanjay V. Patel, Seacoast Science, Inc.,
2151 Las Palmas Dr. Suite C, Carlsbad, CA 92011

STTR Performers: Seacoast Science, Inc. and University of California San Diego

Executive Summary:

Seacoast Science, Inc. and the University of California, San Diego (UCSD) are developing a portable real-time chemical detector system containing multiple sensor technologies. This Phase II STTR final report details our accomplishments during the 2-year program. Scientists at UCSD have modeled the behavior of the metal-phthalocyanine chemFETs, and optimizing both the sensor chemistry and methods to understand the sensor data. Seacoast Science has developed a packed-tube, trap-and-purge preconcentrator to collect vapor samples, with the goal of improving the sensitivity of the ultimate sensor system. Increased sensitivity allows for improved signal to noise for pattern recognition and for better protection for the warfighters who will use the system. In Phase II, Seacoast developed and tested an integrated prototype, integrating both the UCSD chemFET array and Seacoast's chemicapacitor array with the preconcentrator. UCSD has developed methods for solution deposition of sensor films using soluble phthalocyanines. Development of the preconcentrator and sensor materials demonstrate Seacoast's leading-edge sensor systems for chemical threats of critical importance to the US military. Improvements in the systems developed under this program are being integrated into Seacoast's Mini GC product prototypes for vapor detection for applications such as environmental contamination detection and aerosol analysis.

CONTENTS

Section	Page
List of Figures	ii
List of Tables	iii
Acronyms.....	iv
1. Introduction	1
2. Objectives	1
3. Status of Effort.....	1
4. Accomplishments/New Findings.....	2
4.a. ChemFET Materials Development and Optimization.....	2
4.b. Integrated Prototype Development.....	13
4.c. Other Work	24
4.d. Remaining Challenges.....	25
5. Personnel Supported	26
6. Publications	26
7. Interactions/Transitions	26
8. New Discoveries	26
9. Honors/Awards	27

List of Figures	Page
Figure 1. Structure of NiOPc.....	3
Figure 2. I-V Characteristics of CuOPc FET deposited from solution.	3
Figure 3. Chemical sensor response of octabutoxyphthalocyanine sensor 50 nm thick, which has been solution deposited on a chemFET microsensor. Response to dosing to ppmV in air amounts of methanol and dimethylmethylphosphonate (DMMP, a CW agent simulant).....	3
Figure 4. Single crystal structure (Hydrogen atoms and toluene molecules were removed for clarity).	4
Figure 5. Source-drain voltage curve of ChemFET prepared using OBNC films 50 nm thick deposited by spin coating from toluene with the silica gate dielectric covalently modified using a coating of octadecylSi(OMe) ₃ for various coating times.	5
Figure 6. Source-drain voltage curve of ChemFET prepared using OBNC films 50 nm thick deposited by spin coating from toluene with the silica gate dielectric covalently modified using a coating of octadecylSi(OMe) ₃ followed by annealing at 120°C for an hour.	5
Figure 7. Optical Microscope image of H2BuONPc films spray-coated on the OTS modified SiO ₂ /Si TFT chip.	6
Figure 8. Output and transfer characteristics of spray-coated H2BuONPcTFTs: Threshold voltage $V_T = -0.5$ V; mobility $\mu = 0.004 \text{ cm}^2\text{V}^{-1}\text{s}^{-1}$; on/of ratio = 1.6×10^3	6
Figure 9. When a drop of dichloromethane was put onto the spray-coated film, the film became much smoother.	6
Figure 10. Output and transfer characteristics of spray-coated H2BNc TFTs after dichloromethane solvent annealing: Threshold voltage $V_T = -1.8$ V; mobility $\mu = 0.001 \text{ cm}^2\text{V}^{-1}\text{s}^{-1}$; on/of ratio = 5×10^4 . There is a noticeable increase of the on/off ratio but the mobility decreases.	7
Figure 11. Output and transfer characteristics of spray-coated NiBNc TFTs: Threshold voltage $V_T = 0.5$ V; mobility $\mu = 0.002 \text{ cm}^2\text{V}^{-1}\text{s}^{-1}$; on/of ratio = 4.5×10^2	7
Figure 12. UV-Vis absorption spectra of OBNC in solution and thin films. A red-shift of the Q-band λ_{max} is observed for the spin-cast film on glass substrates (887 nm) relative to the solution (864 nm). Annealing the spin-cast film at 120°C for 1 min increased the Q-band red-shift to 918 nm, consistent with increased π overlap in the OBNC J-aggregate structure.....	8
Figure 13. Transfer data for an annealed OBNC TFT stored in ambient air for three weeks.	8
Figure 14. Transient sensing data for vacuum evaporated H ₂ Pc and spin-cast OBNC TFTs exposed to 5min pulses of 160-1600ppmV methanol (MeOH) and 7.6-76ppmV dimethyl methylphosphonate (DMMP). The selectivity of OBNC is improved over H ₂ Pc due to greater than 10× enhanced relative response of DMMP to MeOH.	9
Figure 15. Ultralow power chemFET using thin (15nm) SiNx gate dielectric with transistor and 50nm CuPc film performance shown for low voltage operation.	9
Figure 16. Facile route for synthesis of 1,4-dialkyl-2,3-dicyanonaphthalene and octaalkyl substituted soluble naphthalocyanines.	10
Figure 17. AFM of OTFT film (top), and I-V behavior of octahexylNC complex of Cu(II) (bottom).....	11
Figure 18. Packing of octahexylNC	11
Figure 19. OTFT I-V behavior of ultrathin solution deposited octapentylNC transistor.	12
Figure 20. Linear response of threshold voltage shifts (left panel) for H2Pc, CoPc, and CuPc OTFTs exposed to doses of t-buty peroxide (right panel).	12
Figure 21. Selectivity of preconcentrator materials towards DMMP vs. possible interfering polar compounds (acetone and ethanol).....	14
Figure 22. Metal organic framework (MOF) preconcentrator material showing selectivity towards DMMP vs. possible interferences.	15
Figure 23. (left) 2 nd generation circuit with a parallel flow chamber on top of UCSD's chemFET and Seacoast's chemicapacitive sensor and daughterboard readout circuit inverted on top. (right) PEEK flow cell used to reduce total flow path volume. The arrow shows air flow past active sensing surface for both sensors.....	16
Figure 24. Example sensor responses during preconcentrator cycling test. ChemFET chip #5 (lower) and a chemicapacitor chip #MSS644 (upper) against DMMP.....	16
Figure 25. Schematic of the 4-port, 2-position valve setup. Position A is the preconcentration step and B is the analysis mode.	17

Figure 26. Chemicapacitive sensor array response of four different polymers. 22.6 ppmV DMMP is preconcentrated for 10 min prior to the firing event with simultaneous valve switching to the analysis cycle. The figure shows a series of 5 consecutive preconcentration & analysis cycles of 10 and 1 min, respectively. The Vici Valco 6-port valve used in this setup was heated to about 50°C.....	18
Figure 27. Schematic of two 3-port, 2-position valve setup. Position A is the preconcentration step and B is the detection or analysis mode.....	19
Figure 28. Sensor setup with two miniature 3-port valves from Lee Co. DMMP at 7.9 ppmV was collected for 5, 10, 15, and 20 minutes prior to the preconcentrator firing. The valves were heated to at least 50°C.	19
Figure 29. Sensor setup with two miniature 3-port valves from SMC. DMMP at 7.9 ppmV was collected for 5, 10, 15, and 20 minutes prior to the preconcentrator firing. The valves were heated to about 50°C.	20
Figure 30. Flow rate increase of the sample pump to collect DMMP (7.9 ppmV) on the preconcentrator. The sensor response is plotted as the capacitance change from the HC polymer. The power consumption of the sample pump is shown accordingly.....	20
Figure 31. Preconcentrator test-circuit (left) powered by 8 NiMH (2300mAh) AA-batteries and peak temperature achieved during long-term repeated firing test (right).....	21
Figure 32. Detection results from the new prototype exposed to a constant flow of DMMP (~7.9ppmV) in air powered by a AA 9-Pack of Lithium ion 2700mAh batteries. The batteries powered the system for 5 hours.	22
Figure 33. (left) Schematic of the final circuit board and (right) final Phase II prototype as delivered to UCSD for testing. Case 17 cm x 12 cm x 5.6 cm without AA battery holder.....	22
Figure 34. 7.9ppmV DMMP collected and detected using the new prototype system.	23
Figure 35. Three different chemFETs in the prototype responding to DMMP (stepwise changes).	23
Figure 36. Three chemicapacitors in the prototype responding to the same DMMP steps as in Figure 3.....	23
Figure 37. Principal component analysis of the prototype data collected at UCSD. PC1 and PC2 describe 45.3 and 17.6% of the variance of the data respectively.	24
Figure 38. Two mini-GC chromatograms (HC-chemicapacitor used as the detector) showing repeated collection (shaded boxes) and detection of 20ppbV DMMP in a background of benzene, toluene, and xylene in air.	25

List of Tables	Page
Table 1. LODs estimated from prototype tested in dry air (10-minute collection on preconcentrator)	17
Table 2. Valve types investigated.....	19

Acronyms

ChemFET – Chemically sensitive field effect transistor

DIP – Dual in-line package

DMMP – Dimethyl methylphosphonate (used as a nerve agent simulant)

ERC – Explosive related compound

FOM – Figure of merit

LOD – Limit of detection

MOF – Metal-organic framework

MPc - Metallophthalocyanine

Nc – Naphthalocyanine

OBNc - 5,9,14,18,23,27,32,36-Octabutoxy-2,3-naphthalocyanine

OPc - Octasubstituted phthalocyanines

OTFT – Organic Thin film transistor

OTS – Octadecyltrichlorosilane

Pc – Phthalocyanine

PEEK - Polyetheretherketone

PIM – Polymer of intrinsic microporosity

ppbV – Parts per billion concentration by volume

ppmV – Parts per million concentration by volume

TFT – Thin film transistor

UCSD – University of California, San Diego

1. Introduction

The Phase II STTR program followed two main tracks, ChemFET materials development led by teammates at the University of California, San Diego (UCSD) and system hardware development and testing led by Seacoast Science. UCSD's ChemFET materials development began with vapor deposited (ultrahigh vacuum) films on MEMS structures and transitioned toward use of solution deposition techniques in an effort to more easily and inexpensively fabricate the ChemFET devices. Seacoast's hardware development work involved identifying and integrating system components, redesigning their Phase I preconcentrator control circuitry and integrating the two sensor arrays (chemicapacitor chips and ChemFET chips) into the same flow path. In this report we present the highlights of the entire Phase II program as they relate to these two tracks.

2. Objectives

In Phase I, the team fabricated a multi-detector system that included Seacoast's chemicapacitor sensor array and UCSD's ChemFET array. This approach showed promise to yield a small, portable system with high sensitivity and selectivity to CWAs and explosives related compounds (ERCs). In Phase I the detection of a variety of chemical targets was demonstrated.

The main objective in Phase II was the completion of system integration, system optimization, and the demonstration of the system in field tests with safe simulants at the end of Year 2. Seacoast focused on system integration and optimization tasks related to the preconcentrator and sensors, while UCSD continued their optimization of the Phase I chemFET materials and the development of the statistical modeling of the sensor responses. Seacoast proposed to complete the optimization and integration of the multi-detector preconcentrator platform in Phase II. To accomplish this goal, the following tasks were proposed: preconcentrator material optimization/selection to absorb and retain the specific targets; and integration of Seacoast's chemicapacitive sensor array and resultant optimized preconcentrator with UCSD's ChemFET technology into a seamless unit. Three prototype units for field tests performed by UCSD and for submission to the program manager were completed during the course of the Phase II project.

Phase II Deliverables

A) Scientific and Technical Reporting

A.1 Final Report: This report is submitted to fulfill the requirement.

A.2 Status Reports: Quarterly status reports were submitted during the project.

A.3 Phase II Summary Report: Seacoast submitted an interim summary report at the end of the first project year.

B) Cost Reports: Cost reports were completed as required by the Phase II contract.

C) Additional Reporting: Seacoast prepared additional reports as needed by the program manager.

D) Prototypes: Seacoast has constructed and will deliver three (3) prototypes to the program manager (or other POC) upon completion of the project. The prototypes will include UCSD's chemFET chips, Seacoast's chemicapacitors, and Seacoast's preconcentrator.

3. Status of Effort

Much of the Phase II effort focused on developing improved materials for the ChemFET devices and on integrating the electronics and flow systems to reproducibly control the prototype. While a few of the ChemFET materials were successfully developed into solution cast materials, their long-term stability has not yet been optimized. Similarly, Seacoast investigated a number of preconcentrator sorbent materials, the most promising of which provided significant improvements in sorbent capacity; however,

due to the fact that these materials must operate in air at high temperatures (periodically heated) their long-term viability and reproducibility is still being investigated. Prototypes were constructed using the best available materials at the time. Seacoast tested a number of miniature valves and found most of them had issues such as leaks or incompatible materials of construction that absorbed significant amounts of the target chemicals, making them unsuitable for a fast cycling detection system. Finally, Seacoast developed a power control circuit to manage the heating of the preconcentrator, which is being integrated into it Mini GC prototypes for vapor collection, and is being developed as a stand alone product for Seacoast to market to others doing preconcentrator research and development.

4. Accomplishments/New Findings

4.a. ChemFET Materials Development and Optimization

4.a.1. Device Fabrication, Characterization, and Sensor Testing

ChemFET Structure: Bottom-gate, bottom-contact thin-film transistor (TFT) substrates were fabricated on thermally-grown $\text{SiO}_2/\text{n}^+\text{Si}$ substrates (Silicon Quest). A bi-layer resist lift-off process was used for electrode patterning to minimize the contact resistance. Electrodes composed of a 5nm Ti adhesion layer and 45nm Au were deposited by electron-beam deposition under high-vacuum. The 100nm SiO_2 layer ($C_i=3.45\times 10^{-8}\text{Fcm}^{-2}$) functioned as the gate oxide and the n^+Si as the gate electrode, which was contacted by wet-etching through the SiO_2 and an additional Ti/Au deposition.

Coating Deposition: The TFT substrates were treated with octadecyltrichlorosilane (OTS) by immersion in a 40mM OTS solution in toluene. 5,9,14,18,23,27,32,36-Octabutoxy-2,3-naphthalocyanine (OBNC) thin-films were spin-cast from a 2 % by weight OBNC solution in toluene. The films had a thickness of approximately 50nm as determined by profilometry. For comparison of sensing properties, H_2Pc TFTs were fabricated on untreated substrates using commercial H_2Pc (Aldrich) which had been purified by multiple-zone sublimation. The H_2Pc was evaporated at a rate of 1\AA s^{-1} under ultra-high vacuum (less than 10^{-9} torr) onto substrates held at room-temperature.

I-V Testing: Current-voltage measurements were recorded using an Agilent B1500 semiconductor parameter analyzer. All measurements were recorded under ambient air and at room temperature. The OBNC chips were stored in the dark in ambient conditions to test the device stability. The field-effect mobility, threshold voltage and $I_{\text{on}}/I_{\text{off}}$ ratio were calculated based on the equation for TFT saturation mode operation, $I_d = (WC_i/2L)\mu_{\text{FE}}(V_{\text{gs}} - V_{\text{th}})^2$ where C_i is the gate oxide capacitance, μ_{FE} is the field-effect mobility, V_{th} is the threshold voltage, W is the channel width and L is the channel length.

Measurements during chemical sensing were recorded on a National Instruments PXI-6259 M-Series Multifunction DAQ and controlled by a custom-designed LabVIEW program. The chips were mounted onto a ceramic DIP and drain-current measurements were calculated by recording the voltage drop across a 1.2kOhm resistor. OTFT transfer curves (I_d - V_g) were analyzed every 30 seconds by a gate voltage (V_g) sweep from +10V to -10V at 4Vs^{-1} with the drain voltage (V_{ds}) held at -10V. Transient I_d was plotted for $V_g=V_{\text{d}}=-10\text{V}$. Transient V_{th} and μ_{FE} were calculated. Analyte pulses were introduced to a stainless steel flow chamber using the methods previously reported from this lab.

4.a.2. Solution Processing of ChemFET Sensors

In Phase I we demonstrated the sensing capabilities of various metallophthalocyanines (MPc) deposited from ultra-high-vacuum. This is an expensive method to manufacture arrays, due to costs associated with operating vacuum equipment, processing labor, and the requirement of a vacuum-

compatible masking technique to coat multiple sites on the array with different compounds. Experiments to fabricate chemFETs by solution deposition of sensor films were explored as a way to minimize cost in chemFET fabrication. Soluble octasubstituted phthalocyanines (OPc) of structure shown in **Figure 1** (metal free, Ni(II), Co(II), Cu(II), and Zn(II)) that are known to self organize upon deposition from solution have been spin coated and allowed to crystallize to make microwires on top contact FET devices. These materials show remarkably well-behaved electronic characteristics and appear to be immune to aging effects, which have complicated application of the unsubstituted metal phthalocyanines (MPcs). The structure of a NiOPc is shown in **Figure 1** and the current-voltage behavior of the CuOPc is shown in **Figure 2**.

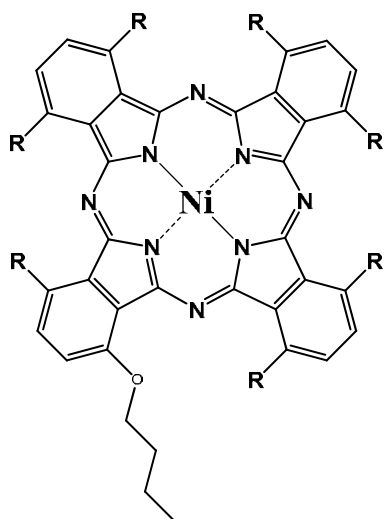


Figure 1. Structure of NiOPc

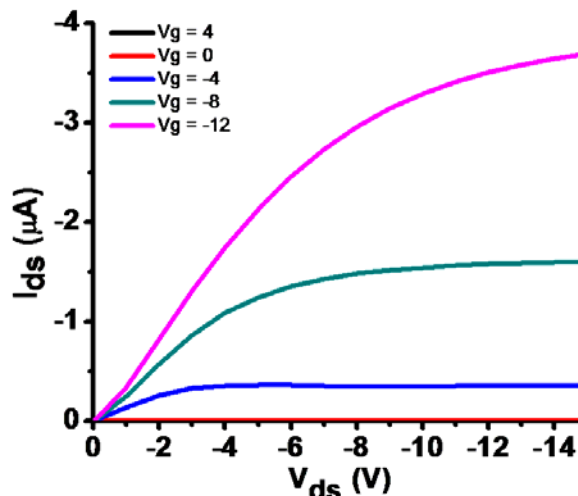


Figure 2. I-V Characteristics of CuOPc FET deposited from solution.

The chemical sensor behavior was characterized (**Figure 3**) and they appear to offer all the advantages of MPc in response with greatly improved sensor stability.

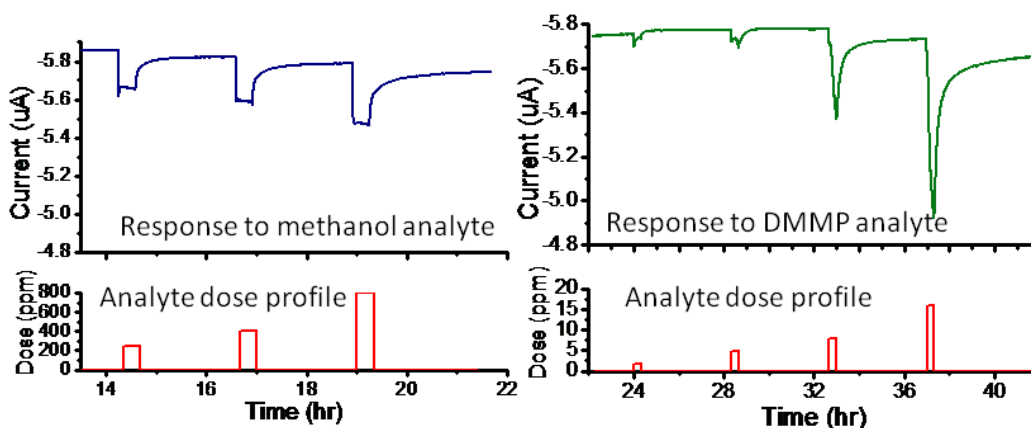


Figure 3. Chemical sensor response of octabutoxyphthalocyanine sensor 50 nm thick, which has been solution deposited on a chemFET microsensor. Response to dosing to ppmV in air amounts of methanol and dimethylmethylphosphonate (DMMP, a CW agent simulant).

A soluble naphthalophthalocyanine, 5,9,14,18,23,27,32,36-Octabutoxy-2,3-naphthalocyanine (OBNc), was synthesized, purified by silica gel column and polymer gel column and recrystallized from toluene-methanol system. OBNc is highly soluble in a range of organic solvents, such as chloroform, toluene and THF. Single crystals of OBNc were grown by slow evaporation of its solution in toluene and it adopts the molecular structure shown below (**Figure 4**).

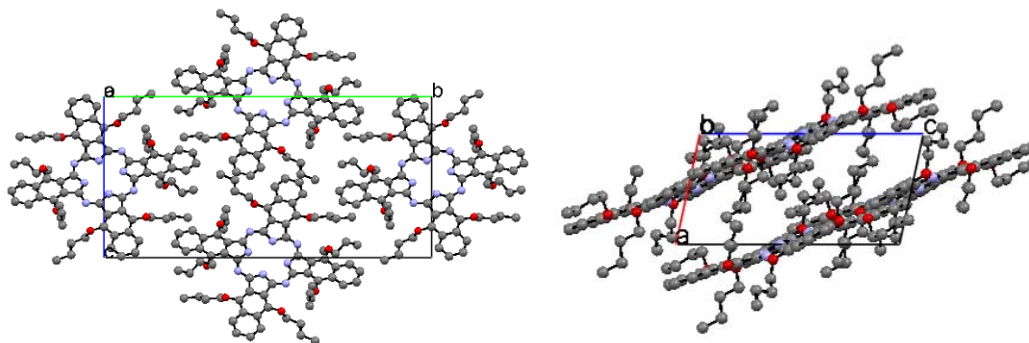


Figure 4. Single crystal structure (Hydrogen atoms and toluene molecules were removed for clarity).

The mobilities of vacuum-deposited Pc films have been found to be in the range of 10^{-5} – 10^{-3} $\text{cm}^2 \text{V}^{-1} \text{s}^{-1}$, while a single-crystal CuPc-based FET afforded the highest mobility of $1.0 \text{ cm}^2 \text{V}^{-1} \text{s}^{-1}$. After treating the SiO_2 gate dielectric of a ChemFET with octadecyl $\text{Si}(\text{OMe})_3$, the spin-coated sensors made using this material exhibit some of the highest conductivities that we have observed for a phthalocyanine or naphthalocyanine device as shown in **Figure 5**. Given the structure of the OBNc crystal, which contains layers of OBNc molecules separated by toluene molecules of crystallization, we postulated that even greater conductivities could be obtained by annealing the films at 120°C to decrease the interplanar spacing to drive away the crystal lattice toluene molecules. The result was an additional order of magnitude increase in conductivity, as shown in **Figure 6**. Aging studies show good stability of the device current and threshold voltages when exposed to ambient atmosphere for over 3 weeks. The chemical sensitivity is excellent, showing enhanced detection for hydrophobic substrates, such as nerve agent stimulants DMMP, over methanol and water. The origin of the enhanced stability toward aging is under investigation. Previous studies suggested that reaction with atmospheric NO_x pollutants led to decay of normal phthalocyanine sensors in ambient air. The enhanced sensitivity toward more hydrophobic reagents may arise from the OBU substituents that form a hydrophobic pocket around the metal binding site.

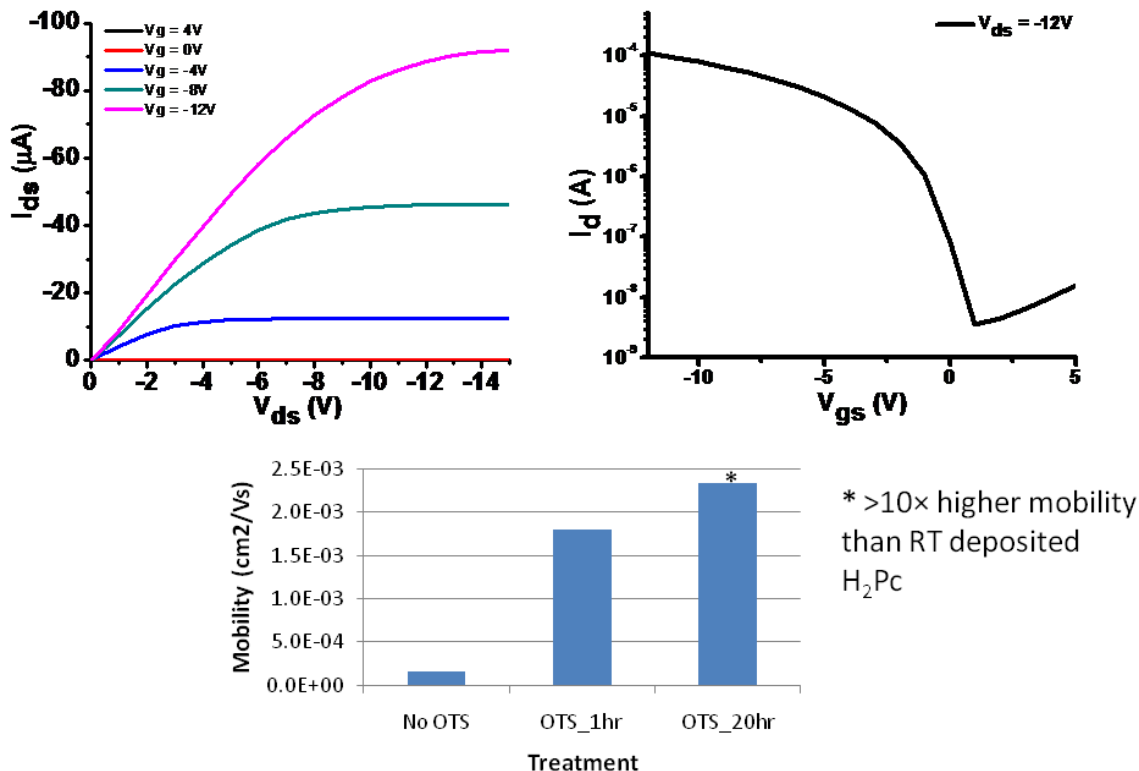


Figure 5. Source-drain voltage curve of ChemFET prepared using OBNC films 50 nm thick deposited by spin coating from toluene with the silica gate dielectric covalently modified using a coating of octadecylSi(OMe)₃ for various coating times.

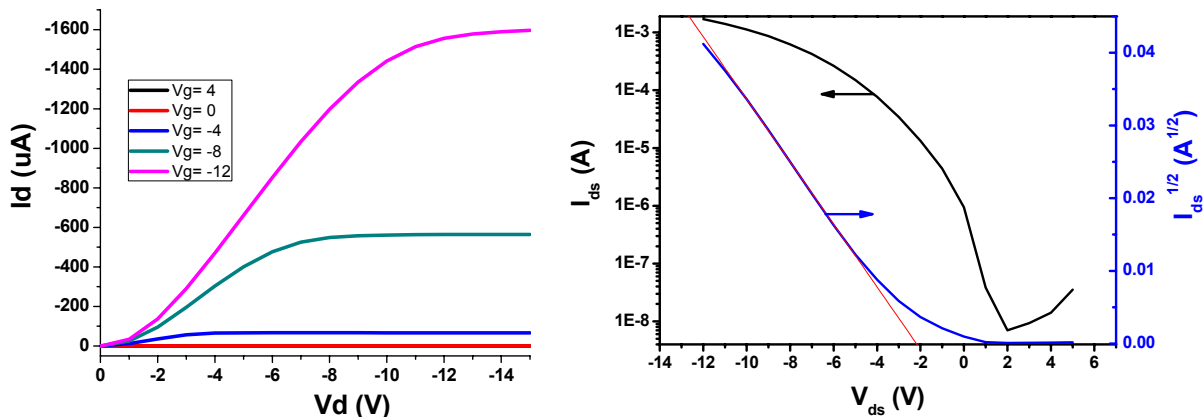


Figure 6. Source-drain voltage curve of ChemFET prepared using OBNC films 50 nm thick deposited by spin coating from toluene with the silica gate dielectric covalently modified using a coating of octadecylSi(OMe)₃ followed by annealing at 120°C for an hour.

We explored the development of spray coating application methods using an airbrush as an alternative to spin-coating application of the sensor films. While spin-coating was very successful, in order to fabricate sensor arrays on a single chip of silicon, spraying using a mask would be a simple method for depositing multiple metal derivatives. Currently we have only been able to fabricate such arrays using time consuming molecular beam methods.

Figure 7 displays an airbrushed H_2OBNC OTFT film airbrushed on an interdigitated electrode array where the semiconducting organic in the channel was deposited over gate oxide treated with octyltrimethoxysilane (OTS) in order to facilitate uniform filling of the channels between the electrodes.

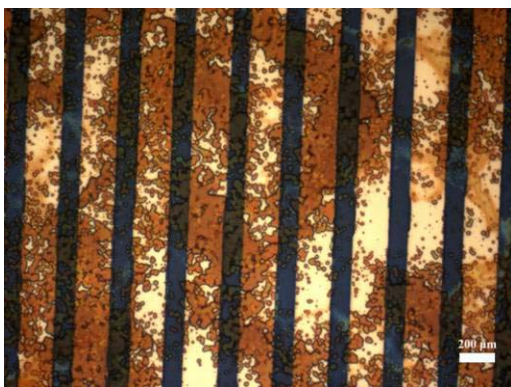


Figure 7. Optical Microscope image of H2BuONPc films spray-coated on the OTS modified SiO₂/Si TFT chip.

While the coating on the metal electrode is visibly non-uniform, filling of the 5 micron channel between the electrodes is uniform enough to create a device with acceptable I-V FET characteristics, as shown in **Figure 8**. Solvent annealing (**Figure 9**) with dichloromethane was explored as a method for improving film uniformity and device performance. Although film uniformity improved, the device electrical performance was not enhanced (**Figure 10**) as compared to the unannealed films.

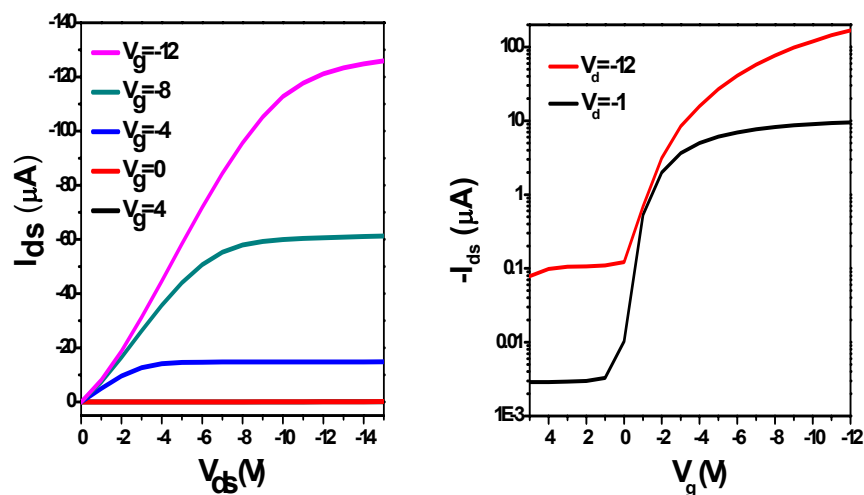


Figure 8. Output and transfer characteristics of spray-coated H2BuONPcTFTs: Threshold voltage $V_T = -0.5$ V; mobility $\mu = 0.004$ cm²V⁻¹s⁻¹; on/of ratio = 1.6×10^3

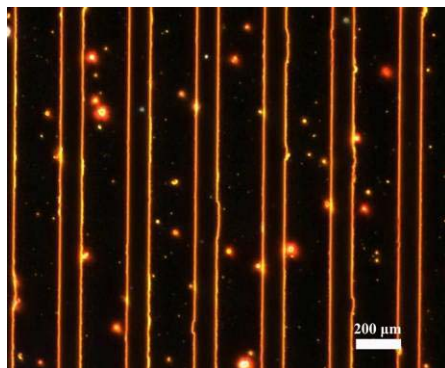


Figure 9. When a drop of dichloromethane was put onto the spray-coated film, the film became much smoother.

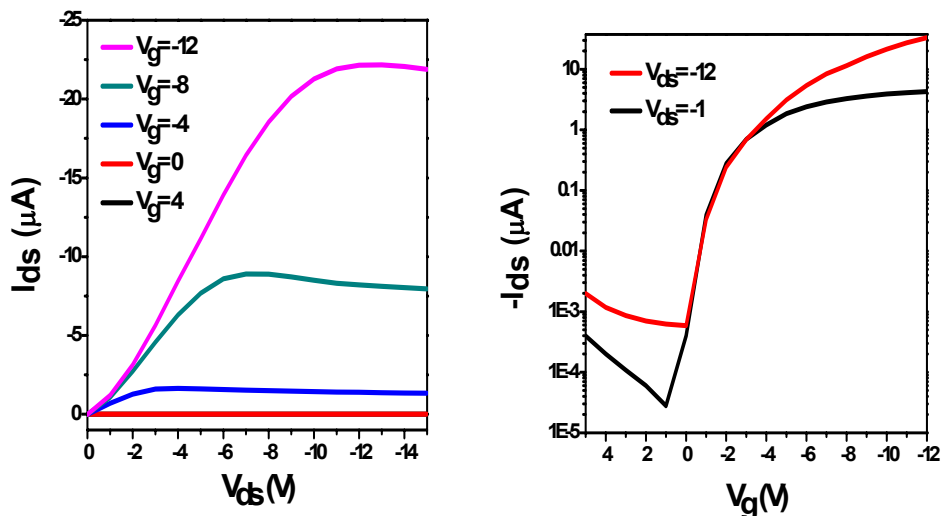


Figure 10. Output and transfer characteristics of spray-coated H2BNc TFTs after dichloromethane solvent annealing: Threshold voltage $V_T = -1.8$ V; mobility $\mu = 0.001 \text{ cm}^2 \text{V}^{-1} \text{s}^{-1}$; on/of ratio $= 5 \times 10^4$. There is a noticeable increase of the on/off ratio but the mobility decreases.

The spray coating method was then tested for a soluble metal naphthalocyanine derivative to see if similar results could be obtained as for the metal free derivative. **Figure 11** shows the electrical characteristics for the corresponding nickel(II) complex, which confirms that the approach should be able to be extended to depositing a variety of soluble conducting sensor films.

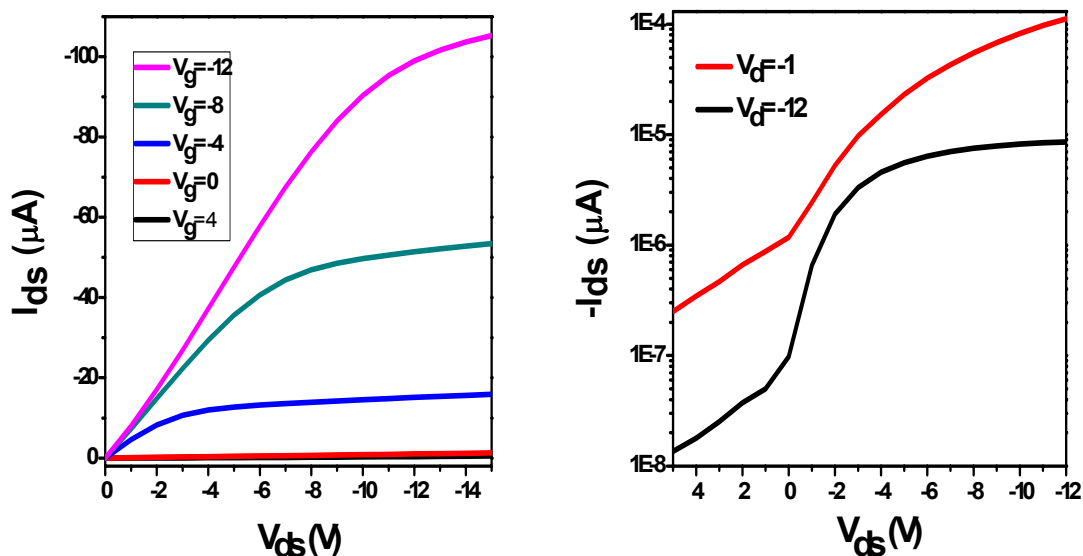


Figure 11. Output and transfer characteristics of spray-coated NiBNc TFTs: Threshold voltage $V_T = 0.5$ V; mobility $\mu = 0.002 \text{ cm}^2 \text{V}^{-1} \text{s}^{-1}$; on/of ratio $= 4.5 \times 10^2$

Spin-coated OBNC films were characterized using UV-Vis spectroscopy, which revealed intermolecular ordering in the thin-film. A red-shift in the OBNC Q-band λ_{max} upon annealing at 120°C suggests improved π - π overlap between adjacent OBNC molecules (**Figure 12**). The λ_{max} red-shift is consistent with the high mobility in annealed OBNC TFTs ($0.06 \text{ cm}^2 \text{V}^{-1} \text{s}^{-1}$), which is more than one order of magnitude larger than the un-annealed OBNC TFTs ($0.004 \text{ cm}^2 \text{V}^{-1} \text{s}^{-1}$). Annealed devices were stored

in ambient air and tested periodically over three weeks with no significant change in mobility and threshold voltage observed (**Figure 13**). The relative sensitivity between strong and weak hydrogen bond acceptor analytes was analyzed with in spin-cast OBNC and vacuum evaporated H₂Pc TFT sensors. The relative sensitivity (**Figure 14**) is over one order of magnitude larger for OBNC, which suggests that the butoxy substituents may serve as peripheral hydrophobic sites to improve sensitivity to strong hydrogen bond acceptors such as the nerve agent stimulant dimethyl methylphosphonate (DMMP) with organic substituents. Thus, the soluble phthalocyanines offer improved stability and sensitivity as long-lived chemical sensor chips.

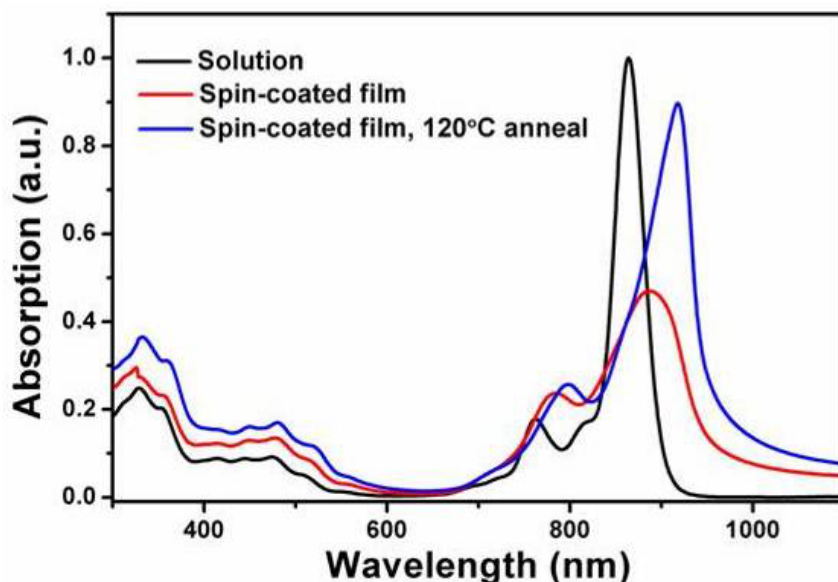


Figure 12. UV-Vis absorption spectra of OBNC in solution and thin films. A red-shift of the Q-band λ_{max} is observed for the spin-cast film on glass substrates (887 nm) relative to the solution (864 nm). Annealing the spin-cast film at 120°C for 1 min increased the Q-band red-shift to 918 nm, consistent with increased π overlap in the OBNC J-aggregate structure.

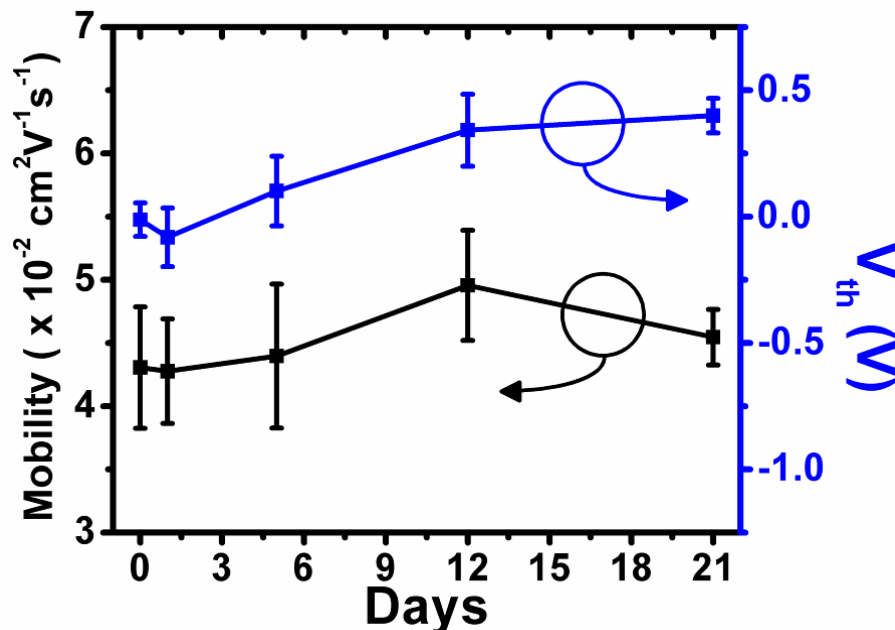


Figure 13. Transfer data for an annealed OBNC TFT stored in ambient air for three weeks.

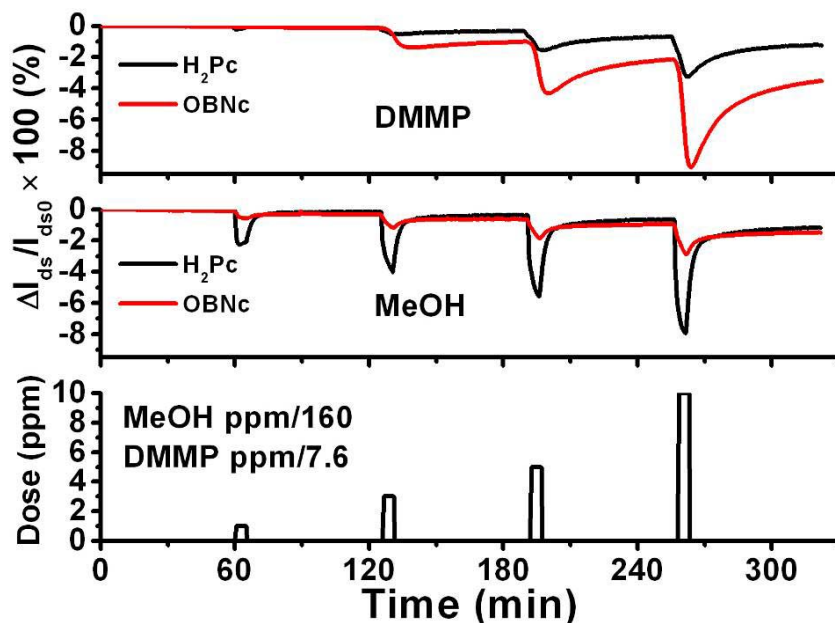


Figure 14. Transient sensing data for vacuum evaporated H_2Pc and spin-cast OBNC TFTs exposed to 5min pulses of 160-1600ppmV methanol (MeOH) and 7.6-76ppmV dimethyl methylphosphonate (DMMP). The selectivity of OBNC is improved over H_2Pc due to greater than 10× enhanced relative response of DMMP to MeOH.

4.a.2. Ultralow Power ChemFET Sensors

In addition to the new process and materials development, ultrathin gate dielectric of SiN_x has been explored so the chemFET sensors can be used in low voltage operation with ultralow power requirements. This work has been carried out with the aid of substrate wafers provided by Qualcomm. The initial results are promising, as shown in **Figure 15**.

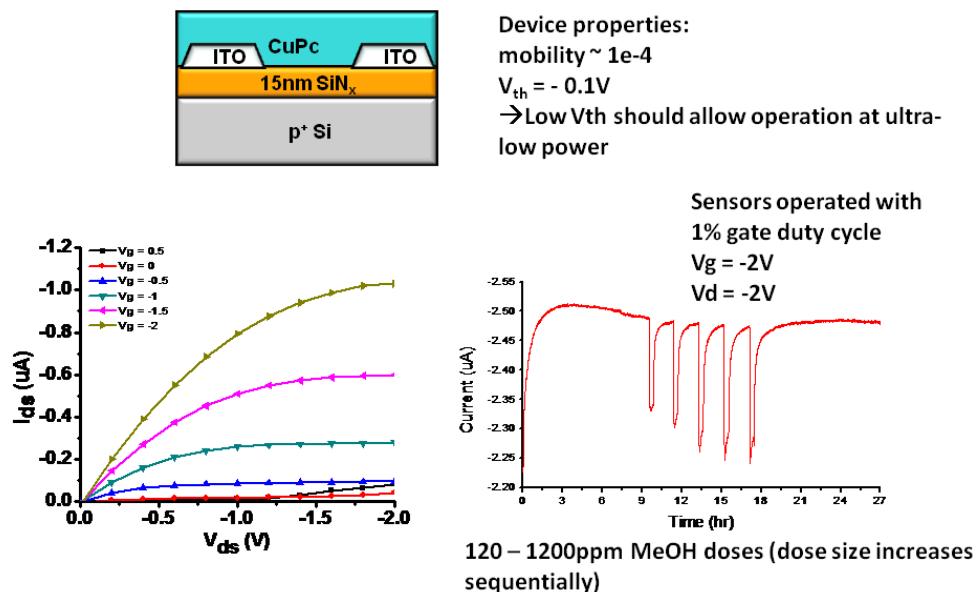


Figure 15. Ultralow power chemFET using thin (15nm) SiN_x gate dielectric with transistor and 50nm CuPc film performance shown for low voltage operation.

4.a.3. New Soluble Alkyl substituted Naphthalocyanine Sensor Materials

Above, we described the use of soluble octabutoxy substituted phthalocyanines (Pc) and naphthalocyanines (Nc) as improved chemical sensor materials. OTFTs fabricated with these materials exhibit 1) reduced drift; 2) resistance to aging and sensor degradation; 3) improved chemical sensitivity. A new class of alkyl substituted Nc derivatives have been synthesized by the new synthetic route described in **Figure 16**.

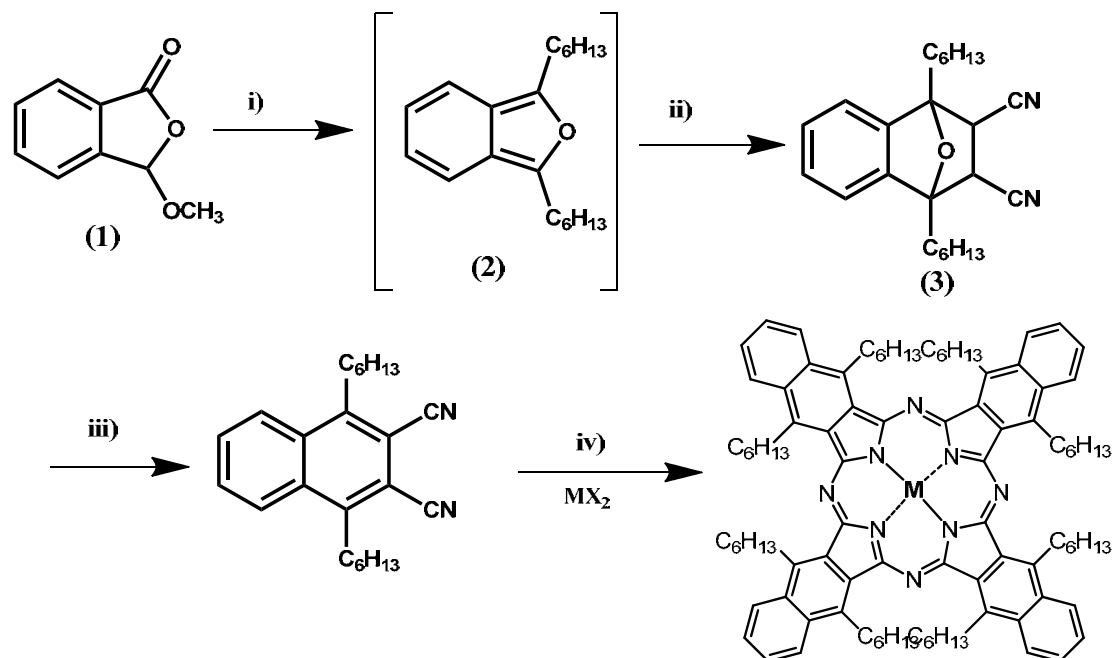


Figure 16. Facile route for synthesis of 1,4-dialkyl-2,3-dicyanonaphthalene and octaalkyl substituted soluble naphthalocyanines.

The overall yield for the three steps to prepare the 1,4-dihexyl-2,3-dicyanonaphthalene is an impressive 34% and this allows the preparation of a wide variety of alkyl substituted derivatives, as shown in Step iv. Both the hexyl and octyl substituted compounds have been prepared: hexyl - ^1H NMR (400 MHz, CDCl_3) δ = 8.17(m, 2H), 7.78(m, 2H), 3.33(t, 4H), 1.73(m, 4H), 1.52(m, 4H), 1.35(m, 8H), 0.90(t, 6H). ^{13}C NMR (400 MHz, CDCl_3) δ = 147.0, 132.7, 130.1, 116.4, 109.9, 32.4, 31.7, 31.3, 29.7, 22.8, 14.3. ESI-MS calculated for $[\text{M-H}]^-$ 345.24, found 345.28; octyl - ^1H NMR (400 MHz, toluene- d_6) δ = 8.79(m, 8H), 7.65(m, 8H), 5.30(s, 16H), 2.17(m, 16H), 2.02 (s, 2H), 1.78(m, 16H), 1.30(m, 20H), 1.14(m, 16H), 0.70(t, 24H). We are characterizing the sensor properties of these new soluble materials and the convenient high yield synthesis makes scale up for commercial production straightforward.

The copper complex has been prepared and OTFTs with the metal free and metal doped materials have been fabricated (**Figure 17**). The structure shows the alkyl chains help orient stacking of the phthalocyanine (**Figure 18**) so that ordered films can be prepared by solvent evaporation rather than expensive MBE methods to yield ~50 nm thick OTFTs of high performance (**Figure 17**).

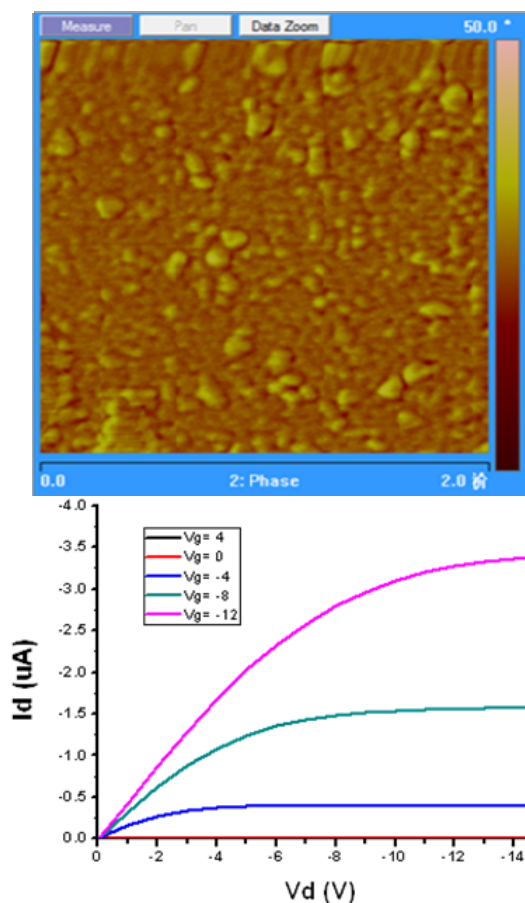


Figure 17. AFM of OTFT film (top), and I-V behavior of octahexylNC complex of Cu(II) (bottom).

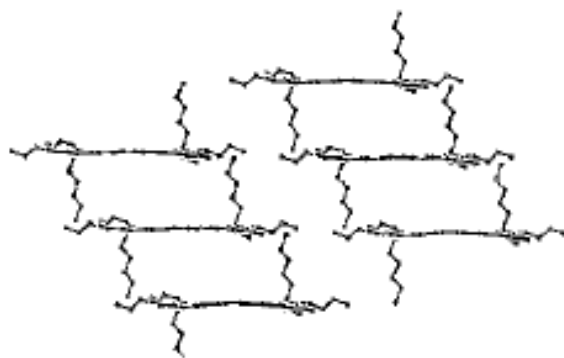


Figure 18. Packing of octahexylNC

The shorter chain octapentyl derivative has been prepared recently and it is surprisingly much less soluble than the octahexyl derivative, which implied much stronger forces in the crystal packing. It was necessary to use supersaturated solutions of the compound in hot toluene to prepare ultrathin OTFTs of high mobility (**Figure 19**). While the low solubility is problematic, it has allowed preparation of the thinnest solution deposited OTFTs so far (AFM characterization in progress).

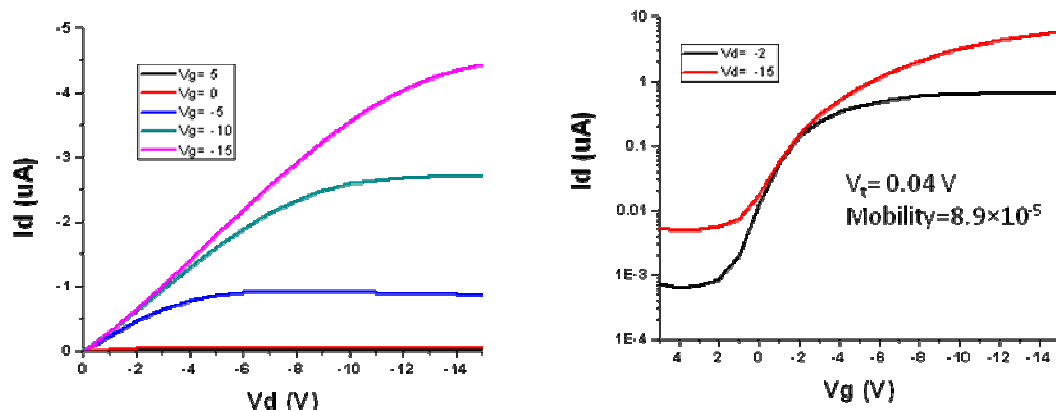


Figure 19. OTFT I-V behavior of ultrathin solution deposited octapentylNC transistor.

4.a.4. Peroxide Sensing with Phthalocyanine Chemical Sensors

Detection of vapor phase hydrogen peroxide (VHP) has numerous applications in the fields of biomedicine and counter terrorism technologies. VHP in expired breath is a marker for acute respiratory failure, as well as acute airway inflammation. Sterilization of medical/pharmaceutical equipment is commonly performed with VHP at concentrations 1000 times above the permissible standard levels set by OSHA for breathable air; therefore, *in-situ* and post-sterilization VHP monitoring is needed for environmental health and safety monitoring in the workplace. Environmental monitoring of organic peroxides and hydroperoxides is required for analysis of harmful tropospheric air pollutants, as well as in ozone-treated drinking water. In the security sector, hydrogen peroxide based explosives are a significant problem because they are readily synthesized from commonly available materials. Methods for peroxide vapor detection include electrochemical, spectrophotometric and chemiluminescence; however, these methods require expensive and bulky instrumentation for continuous monitoring.

The response of 4 ML H₂Pc, CoPc, and CuPc OTFTs exposed to doses of tert-butyl peroxide are presented in **Figure 20**. Each pulse causes an irreversible threshold voltage shift which scales approximately linearly with dose time.

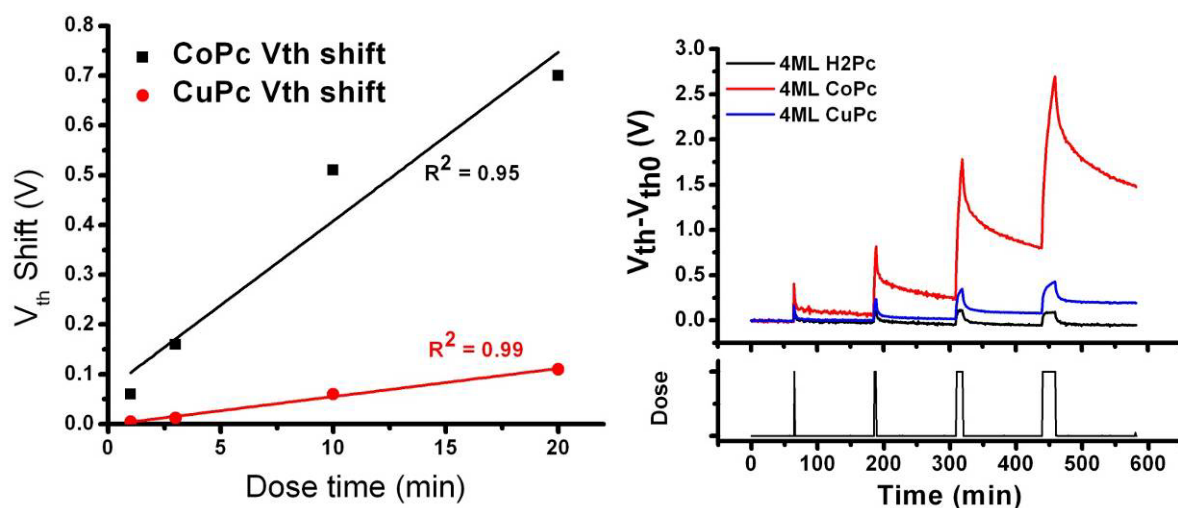


Figure 20. Linear response of threshold voltage shifts (left panel) for H₂Pc, CoPc, and CuPc OTFTs exposed to doses of t-butyl peroxide (right panel).

In this figure, the change in V_{th} is plotted against peroxide dose. The magnitude of the V_{th} shift is linearly proportional to the dose length. The dosimetric response implies that low concentrations of peroxide can be detected by sampling for extended periods of time. The response is characterized by a fast mobility decrease and a dosimetric positive threshold voltage shift. A maximum change in mobility is obtained within five minutes, which is similar for analogous volatile analytes such as water. Conversely, the irreversible threshold voltage shift continues to increase for dose times longer than five minutes. The results are consistent with a mechanism proceeding through molecular chemisorption followed by oxidative decomposition. The peroxide reversibly decreases mobility through molecular chemisorption at the metal center and irreversibly shifts threshold voltage due to oxidative decomposition of the peroxide. This unusual behavior is unique to the peroxide based analytes and offers the possibility for a selective sensor for a broad class of organic peroxides that are being increasingly used in homemade explosives (HME). Extension of these studies to the more stable soluble naphthalocyanine sensors is in progress, and preliminary results suggest up to a 10x increase in sensitivity with the improved sensor materials.

4.b. Integrated Prototype Development

Seacoast's efforts in prototype development focused on developing new sorbent materials for the preconcentrator, and designing and constructing the optimized Phase II prototypes.

4.b.1. Preconcentrator materials

New preconcentrator sorbent materials based on organic bridged polysilsesquioxanes were synthesized for evaluation. In particular, the influence of the organic bridge with the hexafluoroisopropanol was examined. Preconcentrators filled with various materials are connected to the Seacoast chemicapacitive sensors in a prototype circuit and the relative sensor response is used to gauge sorption capability. The capacity of the organic-bridged polysilsesquioxanes was measured against acetone and ethanol interferents. The goal in the preconcentrator material development is not only increasing the effective detection limit of the overall system, but more importantly the *selective* sorption of the target analyte rather than interferents. This preferential sorption will allow not only an increase in the effective sensitivity of the system but also may assist in the back-end processing/pattern recognition, i.e. distinguishing the target analyte from the background. One way to display this relative selectivity is to plot a figure of merit (FOM) as follows:

$$FOM = LOD_{CWA} / LOD_{int} \quad (\text{Equation 1})$$

where LOD_{CWA} is the effective system sensitivity of the preconcentrator material for the target and LOD_{int} is the effective system sensitivity of the same material against the interferent. With these criteria, trends are observed for DMMP (**Figure 21**). The polymer 3STH80 especially shows excellent selectivity (smaller bars) for DMMP in the presence of both acetone and ethanol, than do commercially available adsorbent materials such as Tenax and Porapak P.

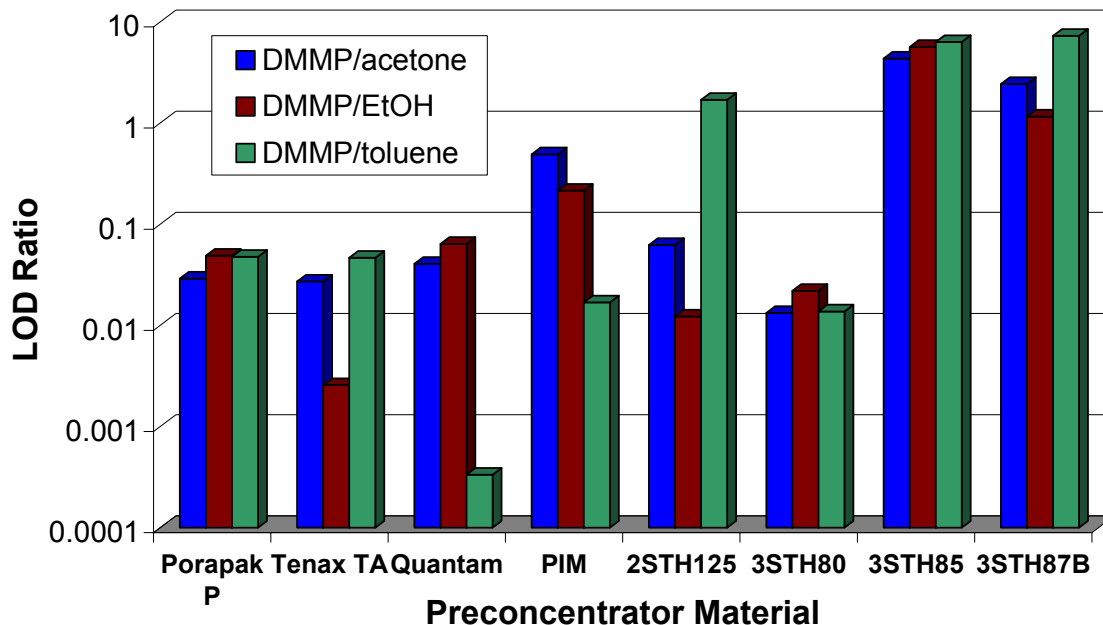


Figure 21. Selectivity of preconcentrator materials towards DMMP vs. possible interfering polar compounds (acetone and ethanol).

Based on the above results, we chose PIM as the preconcentrator material to continue with in this project. It combined thermal stability with selectivity toward DMMP vs. other polar molecules (namely water) and afforded better sensitivity than Tenax (a common sorbent material).

Seacoast also investigated a new type of material for use in the preconcentrator; a novel class of highly microporous and crystalline materials, namely metal organic frameworks (MOF's). These materials have high surface area and tailorable molecular properties to optimize them for a specific application. The crystal lattice of these compounds is constructed by coordination bonds between nodes of metal ions and multidentate organic ligands. The size and functionalization of the ligands can be varied according to its use. Due to the high surface area, lowest reported densities for any crystalline material known to date, tunable pore structure, and high thermal stability, this new class of inorganic-organic materials has attracted widespread attention in gas storage, catalysis, sensing, separation technology, and imaging. However, little work has been done in the research of MOF material used as preconcentrator sorbents.

We synthesized the prototypical MOF-5 structure and evaluated its sorbent behavior in Seacoast's metal capillary preconcentrator. All measurements with the new MOF material were compared with a general Tenax filled preconcentrator for comparison. **Figure 22** shows the results of the sorption study with DMMP, two nitro compounds, three volatile organic compounds (VOC) and water vapor as interferents. Note that the abscissa in the figures is in log scale. Despite the similar mass loading of the preconcentrators, the MOF material shows roughly 10x improvement in the preconcentration for DMMP, the nerve gas simulant, compared to Tenax. More importantly, the inorganic-organic hybrid material shows great selectivity towards the simulant and barely shows any affinity to the other chemicals. Tenax on the other hand, shows only intermediate selectivity with even more affinity towards acetone than the target analyte DMMP. Published results on MOF behavior in humid environments have shown a lack of stability, which led to our omission of the MOF preconcentrators from the prototype systems. Further research is needed to improve their stability in hot humid environments.

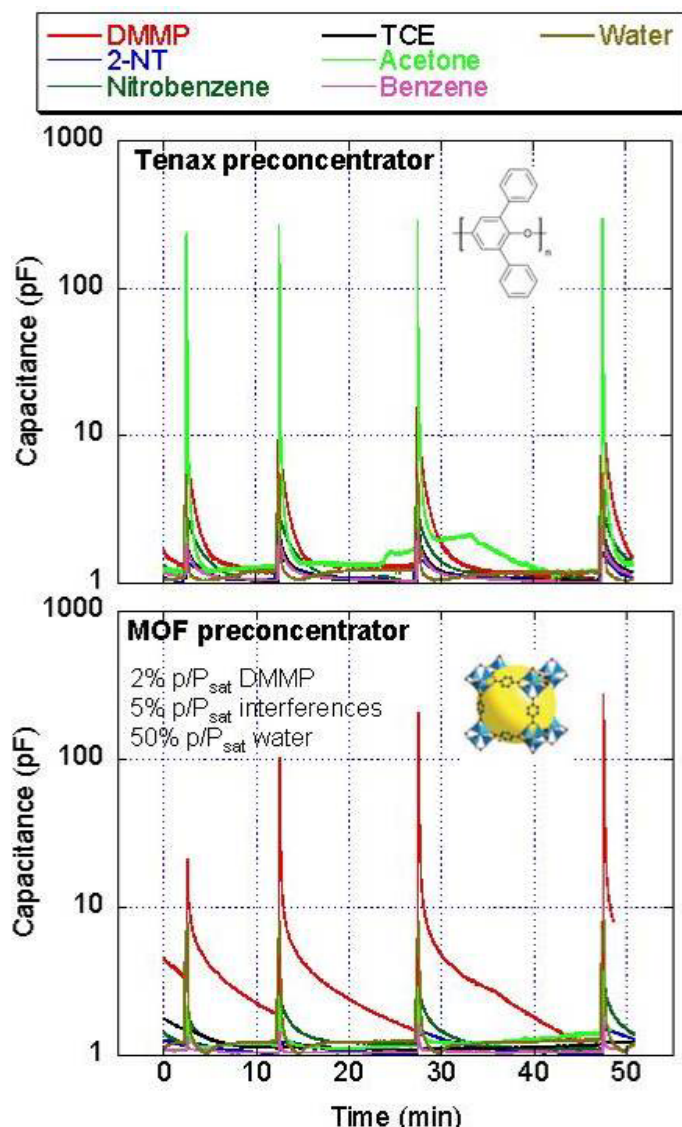


Figure 22. Metal organic framework (MOF) preconcentrator material showing selectivity towards DMMP vs. possible interferences.

4.b.2. Prototype System Development

Seacoast's preconcentrator development progressed on three fronts; 1) optimizing electronic circuitry design, 2) optimizing flow path and related components, and 3) demonstrating portable operation using battery power. In order to develop the prototype and perform testing in parallel, Seacoast used a number of different circuits to perform these tasks.

4.b.2.a. Prototype system designs and testing

Early in the program, Seacoast designed and fabricated two prototype circuits consisting of a preconcentrator, a flow cell containing a Seacoast Science chemicapacitor array and a UCSD chemFET array, a power supply, and operating software. One system (**Figure 23**) was tested in Seacoast's lab and delivered to UCSD for further testing in August 2010. Unlike the Phase I, "1st generation" prototype, where the two sensors were in a series flow path, a new parallel path was designed, and fabricated from PEEK (polyetheretherketone), a hard chemically resistant, thermally stable, non-absorbent polymer.

Seacoast's detector readout was moved to a smaller circuit board attached with a 4-wire cable, and flipped with the sensor facing the UCSD chemFET array chip. This allowed the entire system to be smaller, and allowed for faster sensor responses.

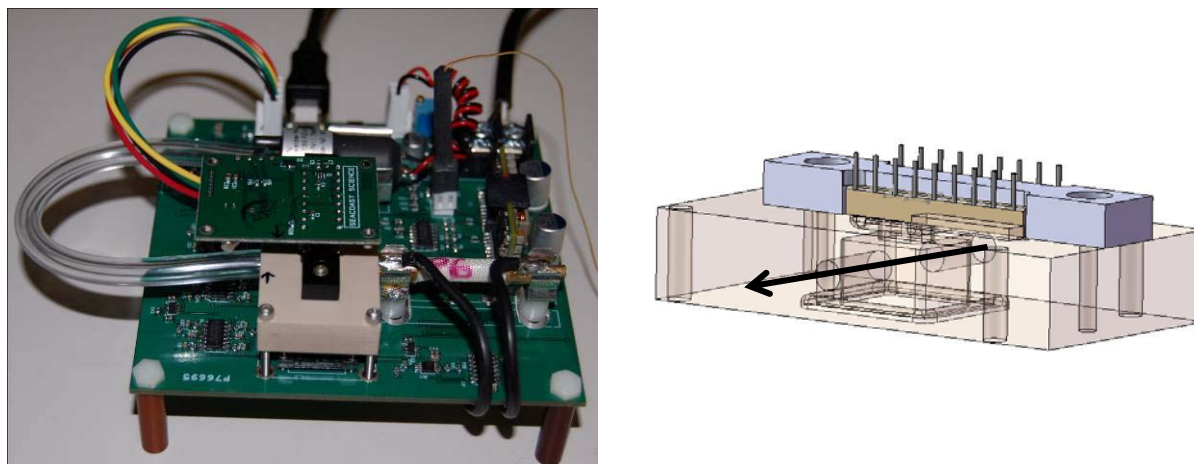


Figure 23. (left) 2nd generation circuit with a parallel flow chamber on top of UCSD's chemFET and Seacoast's chemicapacitive sensor and daughterboard readout circuit inverted on top. (right) PEEK flow cell used to reduce total flow path volume. The arrow shows air flow past active sensing surface for both sensors.

Seacoast used this "2nd generation" prototype to optimize the flow parameters (see below) and system further, while collecting data on different target analytes. For example, **Figure 24** shows the system response during a low-concentration DMMP exposure, with the preconcentrator firing repeatedly (every 5 min). The gradually growing peaks indicate DMMP slowly entering the system. Limits of detection from several of these types of tests are presented in **Table 1**.

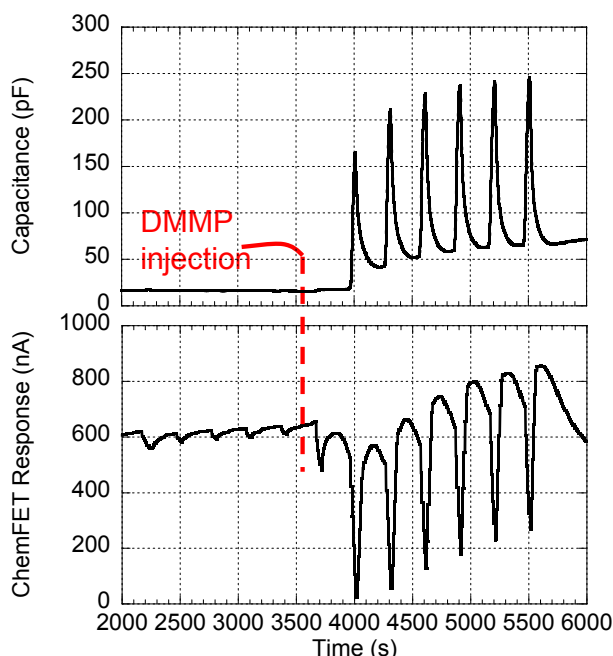


Figure 24. Example sensor responses during preconcentrator cycling test. ChemFET chip #5 (lower) and a chemicapacitor chip #MSS644 (upper) against DMMP.

Table 1. LODs estimated from prototype tested in dry air (10-minute collection on preconcentrator)

Detector type	Chemical exposure and LOD (ppm)			
	DMMP (7.9 ppm)	DIMP (14.8 ppm)	2-Nitrotoluene (2.3 ppm)	Nitropropane (7.3 ppm)
HC Chemicapacitor	0.001	0.002	0.03	0.001
PECH Chemicapacitor	0.05	0.08	0.5	0.1
PEVA40% Chemicapacitor	0.02	0.02	0.04	0.04
H2Pc ChemFET	0.10	0.5	0.9	3

For comparison, the limits of detection (LODs) achieved with HC and the H2PC are 2-3 orders of magnitude better than the inhalation lethal dose ($LC_{50} \sim 17.5$ ppmV-min) for Sarin. A soldier using one of these systems would have at least 35 minutes from first detection (based on 0.5 ppmV H2PC LOD), to don protective gear before reaching the LC_{50} .

Once the valve and pump requirements were determined, a 3rd generation prototype was designed and fabricated and used for the final testing (see below).

4.b.2.b. Flow path development

Seacoast evaluated the use of various valves and flow paths to optimize 1) the collection of vapor samples, 2) the exposure of the sensors, and 3) the clear out (return to baseline) of the sensors. The advantage of an internal switch valve are twofold: (1) the loading of the preconcentrator (environment sampling) can occur at a much higher flow rate using a different pump than the detection event, and (2) while the preconcentrator is being loaded for the next measurement, the sensor and flow path can be purged with clean air to minimize carryover from previous measurements. Switching flow rates to the preconcentrator allows for faster cycling of the entire system, and the ability to purge with clean air allows the sensors to be ready for detection faster, all of which improves sensitivity to target analytes and discrimination over interferences. However, the trade-offs of these additions are (1) increased system power requirements (2) increased system cost (3) possibility of decreased peak height due to the longer flow path through the valves and to the sensors.

Ideally, an inert, small sized 4-port, 2-position valve would suffice for this purpose. A schematic of the valve's function is shown in **Figure 25**. The two valve positions are: (A) preconcentration event for a preset duration; at the same time the sensor is purged with clean air. (B) Analysis cycle starts with thermal desorption (firing) of the preconcentrator to release the analyte towards the sensor.

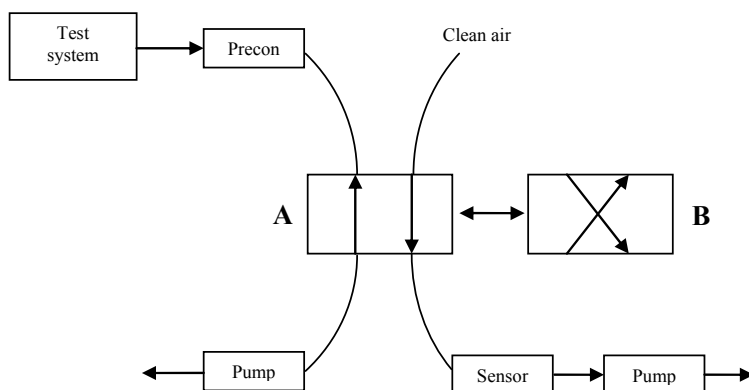


Figure 25. Schematic of the 4-port, 2-position valve setup. Position A is the preconcentration step and B is the analysis mode.

A stainless steel precision valve from Vici Valco Instruments was first used due to the availability of this 6-port valve, commonly used in gas chromatography. The 6-port valve was modified to behave as

a 4-port valve. Although bulky and too pricy for the intended purpose in the sensor system, the Vici valve served as a proof-of-concept of the valve integration. **Figure 26** shows an example of sequential measurement of 22.6 ppmV DMMP. Four different polymers were used in the chemicapacitive sensor array (from top to bottom: PVAC/PEI, HC, PECH, PEVA40%). Each spike corresponds to a firing event after a preconcentration duration of 10 minutes. HC was most responsive to the DMMP analyte. The peak maximum generally occurred about 30 seconds after each firing event. As a consequence, the valve generally remained for 1 min. in position B before switching back to position A, the preconcentration stage.

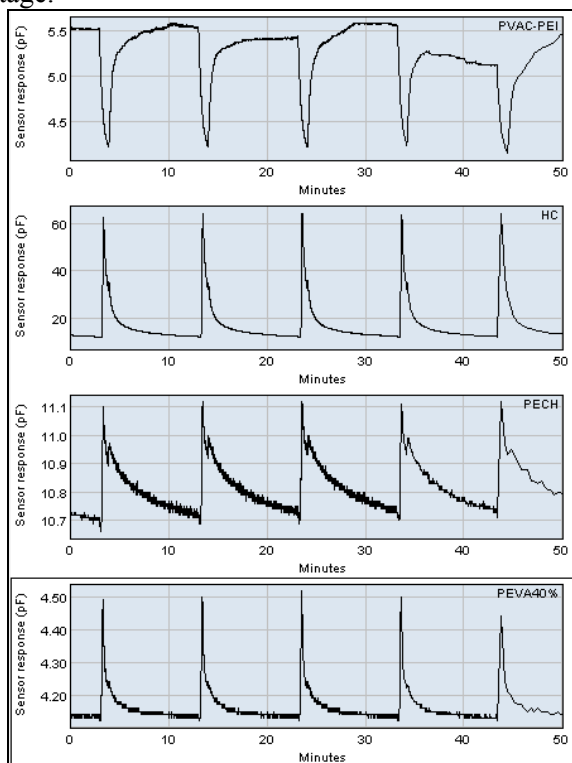


Figure 26. Chemicapacitive sensor array response of four different polymers. 22.6 ppmV DMMP is preconcentrated for 10 min prior to the firing event with simultaneous valve switching to the analysis cycle. The figure shows a series of 5 consecutive preconcentration & analysis cycles of 10 and 1 min, respectively. The Vici Valco 6-port valve used in this setup was heated to about 50°C.

DMMP is considered a sticky analyte due to its low vapor pressure (approximately 0.6 Torr at 15°C). As a consequence, the stainless steel valve required heating to about 50°C with a heating tape. All transfer lines from the preconcentrator to the valve and sensor required either stainless steel or Teflon in order to avoid analyte adsorption.

An extensive search for electrically actuated, small-sized, chemically inert, and temperature resistant 4-port valves turned out to be rather challenging. On the other hand, small-sized 3-way valves are more easily available. As a result, the first alternative to the bulky Vici valve was a combination of two miniature 3-port valves from Lee Co. A schematic of the two 3-port valves setup that we used in the final prototypes is shown in **Figure 27**.

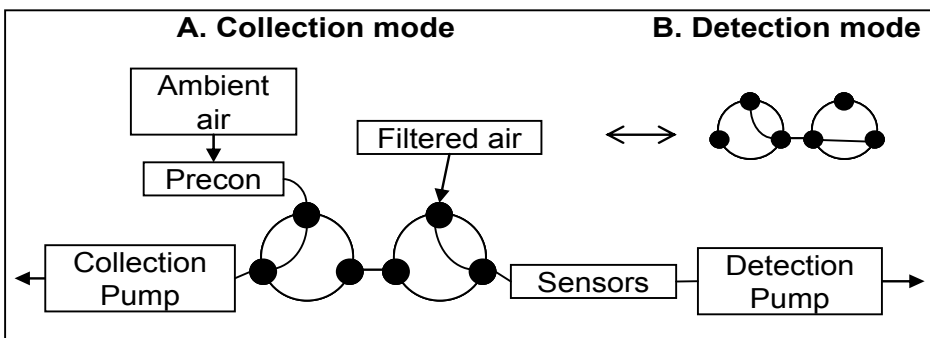


Figure 27. Schematic of two 3-port, 2-position valve setup. Position A is the preconcentration step and B is the detection or analysis mode.

This setup worked well for analytes with a high vapor pressure, such as VOC's like acetone and toluene even at room temperature. However, no signal at all was obtained with DMMP as the analyte. Better results could be collected when the valves were heated to at least 50°C. An example of an experiment with increasing collection time is shown in **Figure 28**. The exposed DMMP concentration for this experiment was lowered to 8 ppmV. The firing event of the preconcentrator (thermal desorption step) was generally set to 5 seconds, corresponding to about 150°C. Increasing the firing time, e.g. preconcentrator temperature resulted in only a minor signal increase.

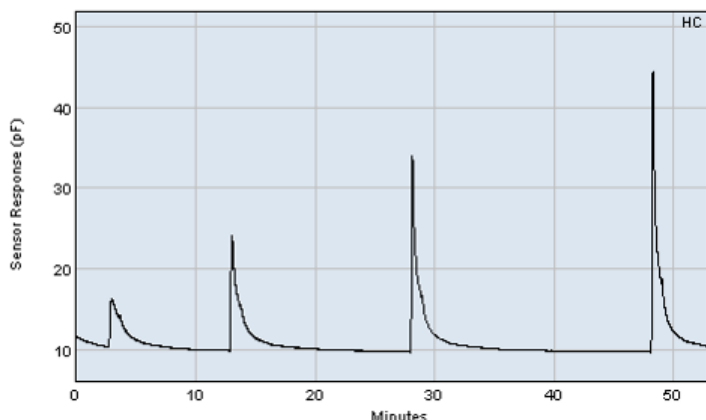


Figure 28. Sensor setup with two miniature 3-port valves from Lee Co. DMMP at 7.9 ppmV was collected for 5, 10, 15, and 20 minutes prior to the preconcentrator firing. The valves were heated to at least 50°C.

The two-valve setup did behave as expected at elevated temperature, producing a larger signal with increased collection time. However, compared to the Vici stainless steel valve or the direct sensor setup without any valves, the two-valve setup was less sensitive to DMMP (decreased peak height at equivalent experimental parameters). The sensitivity decrease with the two valve setup was roughly 50%, likely due to the adsorption of the DMMP onto the valves internal membranes.

Because of the decreased sensitivity with the 'Lee Co' valves different configuration were evaluated with a variety of valves. **Table 2** lists the source and type of all the valves tested, including some small-sized 4-port valves that could be obtained from SMC Corp. of America.

Table 2. Valve types investigated

Manufacturer	Model number	Valve type
Vici Valco Instruments Co	055-1081V	6-port 2-position valve
The Lee Co	496090	3-port 2-position valve
Clippard Instruments	ETO-3-12-V	3-port 2-position valve
SMC Co	SYJ3120-5G-M3	4-port 2-position valve
SMC Co	VQD1151-5L-M5	4-port 2-position valve
SMC Co	S070C-5CG-32	3-port 2-position valve

At room temperature, the use of most of the above listed valves almost completely suppressed the DMMP response due to the adsorption of the analyte along the flow path. All of them are rated up to at least 50°C, at which temperature DMMP was detected by the chemicapacitive sensor, but only to a fraction compared to a sensor system without any valves. The best results were obtained with the valves from ‘SMC Co’. Both the 4-port and 3-port valves show 60-70% of the sensitivity towards DMMP compared to a sensor system without any valves. The 4-port valve had the further disadvantage that it leaked when the valve was actuated, which was not the case with the 3-port valve.

The results in **Figure 29** below show the sensor setup with two SMC 3-port valves.

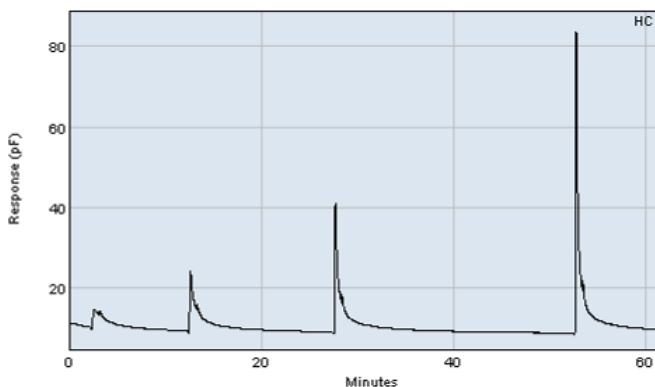


Figure 29. Sensor setup with two miniature 3-port valves from SMC. DMMP at 7.9 ppmV was collected for 5, 10, 15, and 20 minutes prior to the preconcentrator firing. The valves were heated to about 50°C.

As mentioned before, one advantage of having a valve in the system is that a separate sample collection pump can be utilized. This advantage is shown in **Figure 30** where the voltage of the sample collection pump is increased stepwise. The collection time was held steady at 4 minutes (sample exposure: 7.9 ppmV DMMP). The response is measured from the HC polymer sensor and corresponds to the change in capacitance for each preconcentrator firing event at increasing collection flow rate.

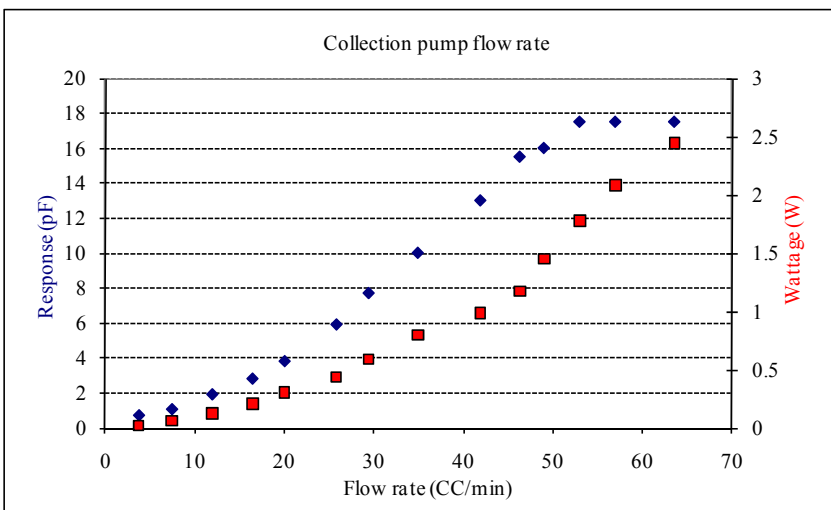


Figure 30. Flow rate increase of the sample pump to collect DMMP (7.9 ppmV) on the preconcentrator. The sensor response is plotted as the capacitance change from the HC polymer. The power consumption of the sample pump is shown accordingly.

We concluded that the SMC 3-way valves in the arrangement above were suitable for the next prototypes. In addition, we tested a number of pumps and found suitable parts for the collection and sampling pumps. The 3rd generation prototypes were designed with the various voltage and power requirements for controlling each of these parts.

4.b.2.c. Battery-power testing

The most significant power usage in the system occurs during the heating of the preconcentrator, when the current draw is on the order of 1 amp, for a few seconds. In contrast, the measurement circuit, pumps and heaters draw about half of that current during the collection periods. Seacoast designed and optimized a preconcentrator control circuit, while the 2nd gen. prototype was being designed and constructed. The circuit replaces the Phase I prototype which used a pulse-width-modulated applied power control circuit, with a DC-DC power converter and a direct application of power to the preconcentrator. The result of this is less noise on the sensors and fewer components in the prototype. This design was implemented on the new prototype.

A preconcentrator test-circuit was connected to a pack of eight AA rechargeable batteries with a nominal (fully charged) voltage of just under 12VDC (**Figure 31**).

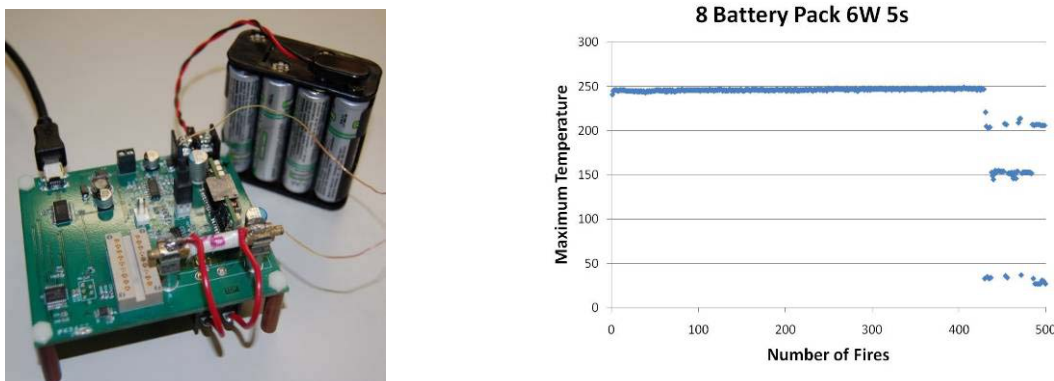


Figure 31. Preconcentrator test-circuit (left) powered by 8 NiMH (2300mAh) AA-batteries and peak temperature achieved during long-term repeated firing test (right).

The control software was programmed to fire the preconcentrator each time its internal temperature reached room temperature, thus operating with the fastest cycle time possible (i.e. the shortest theoretical collection time at room temperature). The software heated the preconcentrator with 6W of power for 5s repeatedly, measuring the temperature each time. The eight AA batteries provided enough power to heat the preconcentrator to full temperature (just under 250°C) 429 times in a row. This test lasted for 12hrs, at room temperature. Although the circuit continued to fire the preconcentrator well past 12 hours, the batteries were no longer able to provide the requested amount of power. Under normal operating conditions, one expects that the collection time would be longer, and therefore the batteries would last longer, however in this test, the power required to operate and control the UCSD and Seacoast sensors was not considered.

Once the valves and pumps had been chosen and the 3rd generation prototype was assembled, we were able to perform a second battery-powered test. **Figure 32** shows the system collecting (10-minute cycle) and detecting DMMP vapors from our laboratory vapor test system for 5-hours on battery power. Nine AA (lithium) rechargeable batteries were used to keep the total voltage at a slightly higher level to accommodate the needs of the heater and pumps. Again, the major power requirements are heating of the preconcentrator during analyte desorption, which needs high currents for short bursts, continuous heating of the valves to keep low-volatility chemicals moving through the system, and continuous operating of the pumps to collect samples and pull air over the sensors.

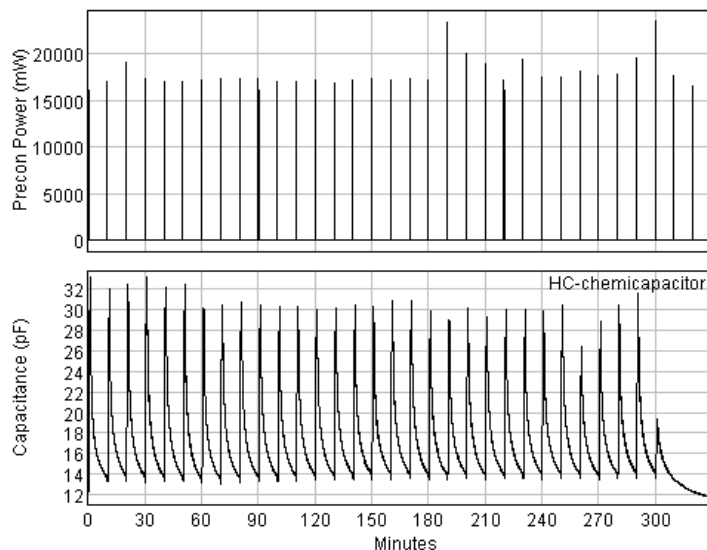


Figure 32. Detection results from the new prototype exposed to a constant flow of DMMP (~7.9ppmV) in air powered by a AA 9-Pack of Lithium ion 2700mAh batteries. The batteries powered the system for 5 hours.

4.b.3. Final Prototype System

Seacoast completed and delivered a 3rd generation prototype system (**Figure 33**) to the UCSD team. This system includes a ChemFET array, a chemicapacitor array, a preconcentrator, and two three-way valves for separate sample collection and sensor purge. The new circuit also contains a heater and valve switching circuitry as well as a 16 bit ACD to increase the resolution of the ChemFET readout.

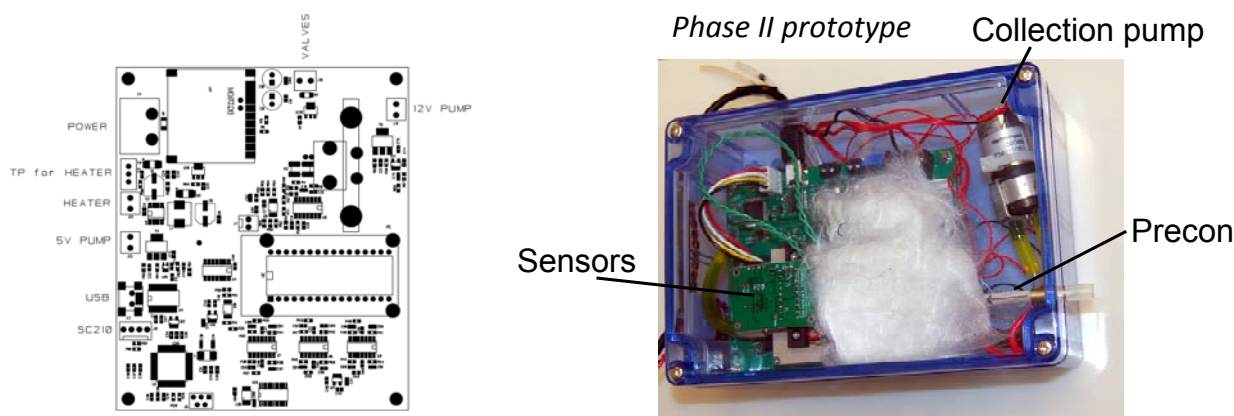


Figure 33. (left) Schematic of the final circuit board and (right) final Phase II prototype as delivered to UCSD for testing. Case 17 cm x 12 cm x 5.6 cm without AA battery holder.

Seacoast is testing various heating methods, optimizing flow paths, and reducing readout circuit noise and measurement timing to improve signal to noise and overall system behavior. **Figure 34** shows the results of a DMMP collection and detection test using the chemicapacitor output to gauge system performance. The inset table shows that with longer collections time detection with the new system matches the behavior we showed in previous reports (i.e. ~ few ppbV detection limits). In essence, we used the heaters and flow rate control to overcome the hindrances of adding length and complexity to the flow path. The improvement in clear out of the sensors allows for faster cycling if needed, and the separation of the collection pump from the sensor flow path, allows for further improvements with larger pumps as needed.

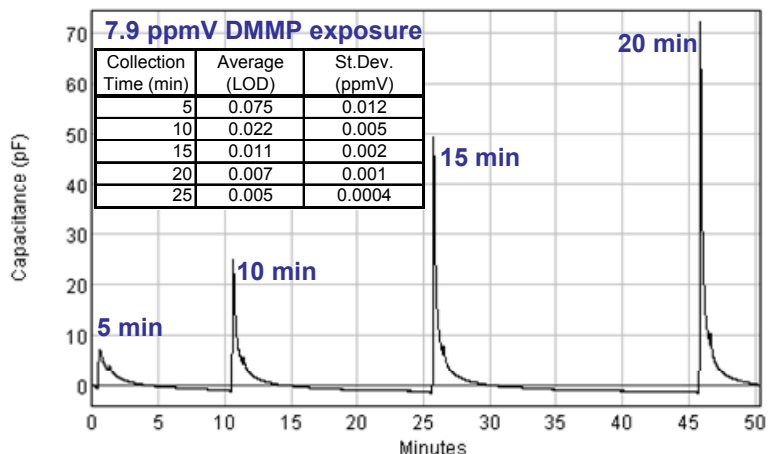


Figure 34. 7.9ppmV DMMP collected and detected using the new prototype system.

One of these systems was delivered to UCSD for testing in their vapor test systems. **Figure 35** and **Figure 36** show data collected by the UCSD students, using the prototype containing the chemFET and chemicapacitor arrays. The DMMP concentration was gradually increased from 0 to 4 times, resulting in 4 increasing responses until ~1300 s when the DMMP was removed and the responses decrease.

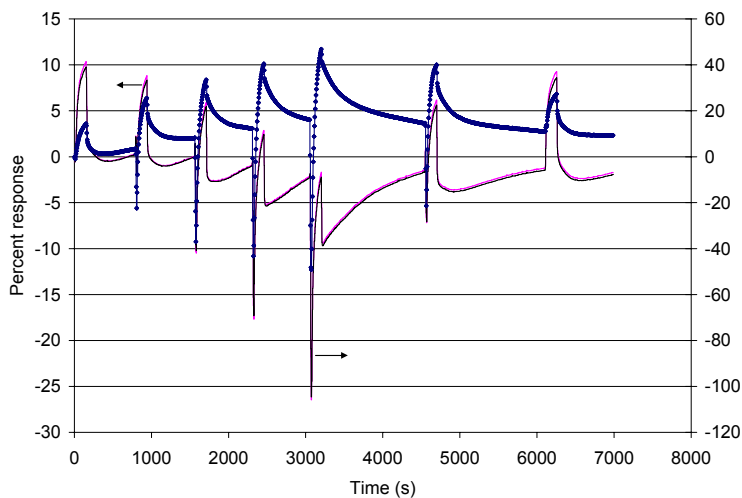


Figure 35. Three different chemFETs in the prototype responding to DMMP (stepwise changes).

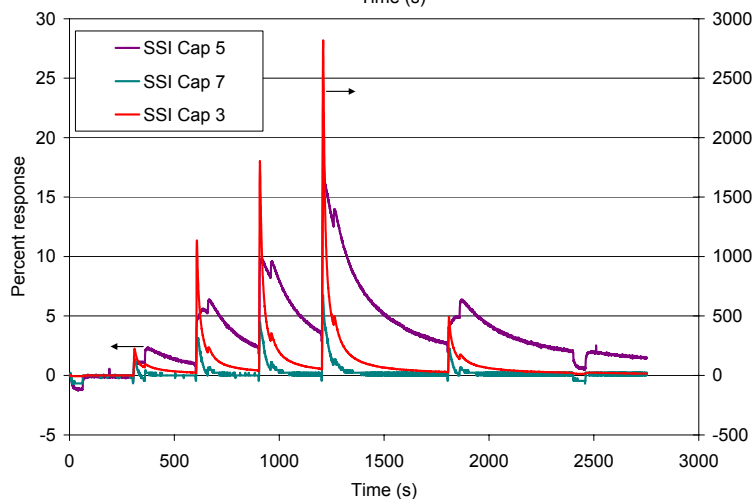


Figure 36. Three chemicapacitors in the prototype responding to the same DMMP steps as in Figure 3.

Data collected in the above tests were analyzed using principal component analysis (ProStat, V. 5.03, Poly Software International, Inc. Pearl River, NY). The peak (or valleys) responses from each of the differently coated sensors (3 chemFETs and 4 polymer chemicapacitors) were normalized by a scaling factor (standard deviation of all responses for each particular sensor). The plot in **Figure 37** of the resulting data shows that the responses from each of the exposed chemicals are clustered and distinct when plotted in the principal component (PC) space. Further data should be collected over a range of different conditions to completely model the expected operational space.

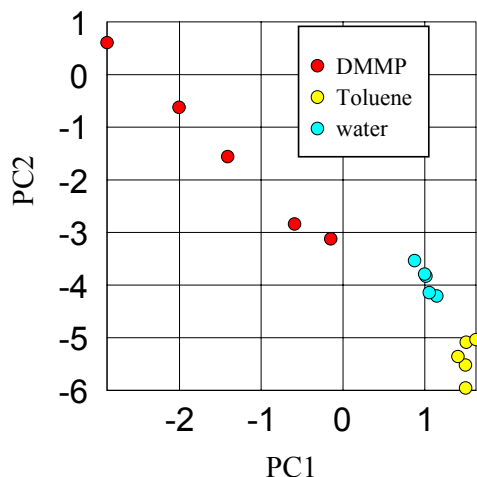


Figure 37. Principal component analysis of the prototype data collected at UCSD. PC1 and PC2 describe 45.3 and 17.6% of the variance of the data respectively.

4.c. Other Work

Over the course of the Phase II project, Seacoast constructed and delivered two prototype systems to teammates at UCSD for testing and data collection. In addition, Seacoast and UCSD presented posters at AFOSR annual reviews in Boston (2010) and Arlington (2011), and supported the AFOSR by providing program summary slides during the project.

For another project, Seacoast has successfully integrated the same preconcentrator circuitry used in the current program into a prototype vapor collection Mini-GC. **Figure 38** shows two chromatograms from a Mini-GC exposed to 20ppbV of DMMP in an overwhelming background of benzene, toluene, and xylene (~277, 71, 18ppmV, respectively). DMMP is successfully separated and detected using a HC-coated chemicapacitor, at well above 3x noise, in approximately 6.5-minutes. This is well below the OSHA Acute Exposure Guideline Levels (AEGL-3, 64 ppbV for 10 min exposure) and almost 1000 below the Lethal Dose Inhalation (LC_{t50} ~ 17.5 ppmV-min) for Sarin.

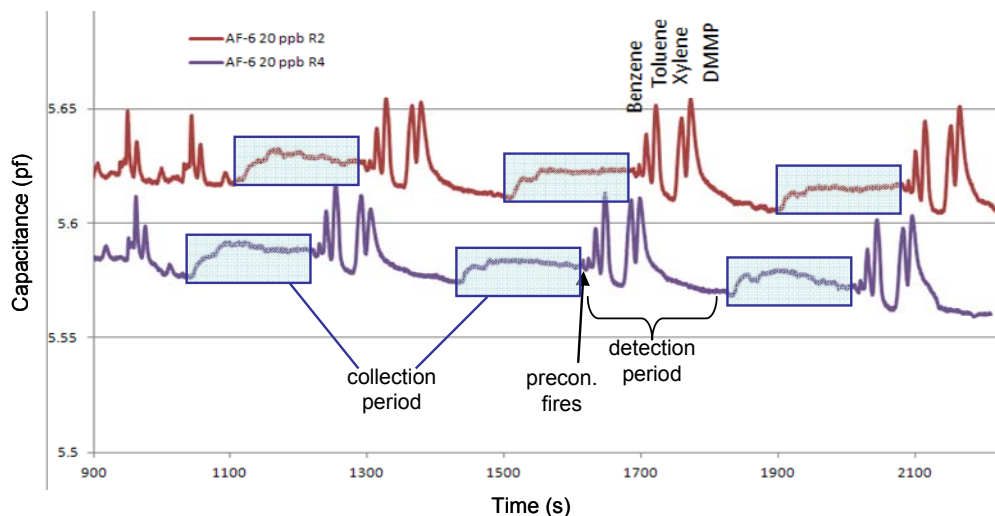


Figure 38. Two mini-GC chromatograms (HC-chemicapacitor used as the detector) showing repeated collection (shaded boxes) and detection of 20ppbV DMMP in a background of benzene, toluene, and xylene in air.

4.d. Remaining Challenges

During the course of the project we noted that a number of challenges still remain before these technologies can be successfully commercialized; some are straightforward engineering issues, while others require further scientific research. These include:

- Reducing power requirements to reduce maintenance cycles
- Integration of a user-interface with the system to reduce the number of system components
- Reducing chemFET drift rate to allow for longer system life
- Extensive live chemical agent testing to collect performance and training data
- Completion of pattern recognition algorithms based on live agent tests and interferences

Seacoast's choice to implement a dual pump and valve system for increased sample collection efficiency was a trade-off against power and system complexity (requirement of heaters and extra circuitry). Reducing the pressure drop across the preconcentrator and improving the materials of construction of the valves would reduce the power requirements. Further research on the thermal and moisture stability of the preconcentrator materials is also required to determine their ultimate lifetimes. This is especially crucial for chemical targets which have lower volatility than G-agents, i.e. explosives. Progress toward simplifying chemFET materials deposition using soluble materials vs. evaporated films has shown a path to improved sensitivity and sensor life. However poisoning issues still need to be resolved for the phthalocyanine materials before the chemFETs can be commercialized.

Even with these issues remaining, Seacoast sees great potential for the technology development that has resulted from this work. UCSD has published its chemFET materials development work (see below) and Seacoast is progressing with commercialization of the preconcentrator technology as an independent platform-agnostic technology. In addition, as shown above, it has already been integrated into our newest mini-GC prototypes and used for vapor collection and detection.

5. Personnel Supported

At Seacoast:

Dr. Sanjay V. Patel
Dr. Marcel Benz
Dr. William Tolley
Dr. Stephen Hobson
Ms. Sabina Cemalovic
Ms. Janet Thieme
Mr. Venko Gyokov

At UCSD:

Dr. William Trogler
Dr. Andrew Kummel
Dr. Ivan Schuler
Dr. Chengyi Zhang (post-doc)
Mr. James Royer (graduate student)
Mr. Eric Kappe (graduate student)

6. Publications

1. "Air-Stable Spin-coated Naphthalocyanine Transistors For Enhanced Chemical Vapor Detection" Author(s): Royer, James; Zhang, Chengyi; Kummel, Andrew; Trogler, William. *Langmuir*, accepted.
2. "Organic Thin-Film Transistors for Selective Hydrogen Peroxide and Organic Peroxide Vapor Detection," Author(s): Royer, James; Zhang, Chengyi; Kappe, Eric; Kummel, Andrew; Trogler, William, in preparation.
3. Analyte selective response in solution-deposited tetrabenzoporphyrin thin-film field-effect transistor sensors, Royer, J. E., Lee, S., Chen, C., Ahn, B., Trogler, W. C., Kanicki, J., Kummel, A. C., *Sensors Actuators B: Chem.*, 158, 333-339 (2011)
4. A final publication on alkyl substituted naphthalocyanine OTFT sensors is planned.

7. Interactions/Transitions

Explored applications to explosives/IED detection of OTFTs with Dr. Noel Janda, Intel Capital, SATO America, DSI, Inc. that would also involve integration of UCSD detectors and Seacoast Science, Inc.

Explored new mass fabricated ITO electrode on SiN OTFTs produced by Qualcomm as a less expensive OTFT platform for sensors.

8. New Discoveries

Air-stable organic thin-film transistor (OTFT) sensors fabricated using spin-cast films of 5,9,14,18,23,27,32,36-octabutoxy-8 2,3-naphthalocyanine (OBNc) demonstrated improved chemical vapor sensitivity and selectivity relative to vacuum-deposited phthalocyanine (H₂Pc) OTFTs. UV-vis spectroscopy data show that annealed spin-cast OBNc films exhibit a red-shift in the OBNc Q- band λ_{max} which is generally diagnostic of improved π -overlap in phthalocyanine ring systems. Annealed OBNc OTFTs have mobilities of $0.06 \text{ cm}^2 \text{ V}^{-1} \text{ s}^{-1}$, low threshold voltages ($|V_{\text{th}}| < 1 \text{ V}$), and on/off ratios greater

than 10^6 . These air-stable device parameters are utilized for sensing modalities which enhance the sensitivity and selectivity of OBNC OTFTs relative to H₂Pc OTFTs. While both sensors exhibit mobility decreases for all analytes, only OBNC OTFTs exhibit V_{th} changes for highly polar/nonpolar analytes. The observed mobility decreases for both sensors are consistent with electron donation trends via hydrogen bonding by basic analytes. In contrast, V_{th} changes for OBNC sensors appear to correlate with the analyte's octanol–water partition coefficient, consistent with polar molecules stabilizing charge in the organic semiconductor film. The analyte induced V_{th} changes for OBNC OTFTs can be employed to develop selective multiparameter sensors which can sense analyte stabilized fixed charge in the film to provide a new sensing modality in OTFTs, which has been applied to peroxide sensing.

MPc and OBNC based OTFTs exhibit irreversible threshold voltage shifts on exposure to hydrogen peroxide, and tert-butyl hydroperoxide. By sensing at gate voltages near the V_{th} (the subthreshold regime) the $\Delta I_{ds}/I_{ds0}$ response is greatly enhanced and the sensitivity to peroxide analytes increases. The sensor response is positive and irreversible in both $\Delta I_{ds}/I_{ds0}$ and V_{th} whereas the mobility response is negative and reversible. The dual response for peroxide sensing suggests a mechanism in which chemisorption reversibly reduces mobility, followed by redox cleavage of the peroxide bond inducing fixed positive charge and positive threshold voltage shifts. These sensors are therefore selective to peroxide and present unique practical advantages over competing technologies. These discoveries have been submitted for publication as listed in Section 6.

9. Honors/Awards

None